Chapter 3

Local and Global Error Analysis

In this chapter we state and prove new superconvergence results for DG solutions on triangular elements. It is well known that if h denotes mesh size, the local discretization errors of piecewise polynomial of degree p DG solutions converge at an $O(h^{p+1})$ rate. We present several new $O(h^{p+2})$ pointwise superconvergence results for the three types of elements and three polynomial spaces. In particular, we show that the solution on elements of type I is $O(h^{p+2})$ superconvergent at the two vertices of the $inflow$ edge using the space $\mathcal{U}_p$. On elements of type II, the DG solution is $O(h^{p+2})$ superconvergent at the Legendre points on the $outflow$ edge as well as at interior mesh orientation dependent points. On elements of type III , the DG solution is $O(h^{p+2})$ superconvergent at the Legendre points on the $outflow$ edge and for the space $\mathcal{U}_p$ the DG solution is $O(h^{p+2})$ superconvergent at every point of the $outflow$ edge. We also proved the existence of several interior superconvergence points.

We first introduce the DG method and we derive the weak formulation for the DG method for the three model problems followed by a convergence analysis. The main results of this chapter consist of proofs of the superconvergence results for the local and global errors. We limit our discussion to scalar hyperbolic problems and begin with the linear model problem.

3.1 DG Formulation and Preliminary Results

We consider a linear two-dimensional first-order hyperbolic conservation law (transport equation) on a bounded convex polygonal domain $\Omega \subseteq R^2$. Let $\boldsymbol{a} = [\alpha, \beta]^T$ denote a constant unit velocity vector (characteristic direction). If $\boldsymbol{n}$ denotes the outward unit normal vector, the domain boundary $\partial\Omega = \partial\Omega^+ \cup \partial\Omega^- \cup \partial\Omega^0$, where

$\partial\Omega^- = \{(x,y) \in \partial\Omega \mid \boldsymbol{a}.\boldsymbol{n} < 0\}$, is the $inflow$ boundary,
$\partial\Omega^+ = \{(x,y) \in \partial\Omega \mid \boldsymbol{a}.\boldsymbol{n} > 0\}$, is the $outflow$ boundary and
$\partial\Omega^0 = \{(x,y) \in \partial\Omega \mid \boldsymbol{a}.\boldsymbol{n} = 0\}$, is the characteristic boundary.

Let $u(x,y)$ denote a smooth function on Ω and consider the following hyperbolic problem (transport-reaction equations):

$$\boldsymbol{a}.\nabla u + cu = \alpha u_x + \beta u_y + cu = f(x,y), \quad (x,y) \in \Omega = [0,1]^2, \tag{3.1a}$$

subject to the boundary conditions

$$u(x,0) = g_0(x), \quad u(0,y) = g_1(y), \tag{3.1b}$$

where the functions $f(x,y)$, $g_0(x)$ and $g_1(y)$ are selected such that the exact solution $u(x,y) \in C^\infty(\Omega)$. Let c, $\alpha \geq 0$, $\beta \geq 0$, $\alpha^2 + \beta^2 > 0$, be real constants. We chose this problem only for the sake of clarity and simplicity. All the results we obtain can be easily extended to hyperbolic problems of the form (1.5) and (1.7).

In order to obtain the weak DG formulation for problem (3.1), we partition the physical domain $\Omega = [0,1]^2$ into a regular mesh having N triangular elements (non-overlapping triangular elements) $\Delta_j, j = 1, ..., N$, of diameter $h > 0$, and assume, for simplicity, that this can be done without error. Clearly there will be N elements such that $\bigcup_{j=1}^{N} \overline{\Delta_j} = \overline{\Omega}$, where $\overline{\Omega}$ denotes the closure of Ω. Furthermore, two elements Δ_i and Δ_j can intersect at a single vertex, along a single edge, or not at all.

Our DG method is constructed on meshes having triangular elements as shown in Figure 3.1. Thus an element will consist of three distinct components or modes: vertex modes, edge modes, and interior modes.

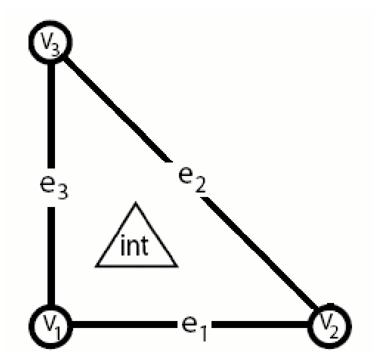

Figure 3.1: A triangular element with its components labeled.

We begin the development of the DG method by first approximating u by a piecewise polynomial function U whose restriction U_j to $\Delta_j, j = 1, ..., N$ is an element of $\mathcal{P}_p(\Delta_j)$ consisting of complete polynomials of degree p in two-dimensions. Here $U_j(x,y)$ is the piecewise polynomial not necessarily continuous across inter-element boundaries. In the remainder of this thesis we omit the element index and refer to an arbitrary element by Δ whenever confusion is unlikely.

Let us multiply (3.1a) by a test function $v(x, y)$, integrate over an arbitrary element Δ, we obtain the associated variational formulation which consists of finding u such that

$$\iint_\Delta (\boldsymbol{a}.\nabla u + cu)v dxdy = \iint_\Delta f v dxdy. \tag{3.2}$$

Next we apply Green's theorem to obtain

$$\int_\Gamma \boldsymbol{a}.\boldsymbol{n}uv ds + \iint_\Delta (-\boldsymbol{a}.\nabla v + cv)u dxdy = \iint_\Delta f v dxdy, \tag{3.3}$$

where $\boldsymbol{n}$ is the unit outward normal to Γ. We decompose the $inflow$ boundary Γ of Δ into $inflow$ edges Γ^- and $outflow$ edges Γ^+ so that $\Gamma = \Gamma^- \cup \Gamma^+$. With this, equation (3.3) becomes:

$$\int_{\Gamma^-} \boldsymbol{a}.\boldsymbol{n}uv ds + \int_{\Gamma^+} \boldsymbol{a}.\boldsymbol{n}uv ds + \iint_\Delta (-\boldsymbol{a}.\nabla v + cv)u dxdy = \iint_\Delta f v dxdy. \tag{3.4}$$

Next we approximate $u(x, y)$ by a piecewise polynomial function $U(x, y)$ whose restriction to Δ is in $\mathcal{P}_p$. Let $S^{N,p}$ denote the space of piecewise polynomial functions U such that the restriction of U to an element Δ is in $\mathcal{W}_p$ which denotes $\mathcal{P}_p$, $\mathcal{V}_p$, or $\mathcal{U}_p$.

For hyperbolic problems, we know that solution information propagates along characteristic lines. Thus, in order to determine the solution on the active element Δ we only need the flux on the $inflow$ edges of Δ. The discrete DG formulation consists of determining $U \in S^{N,p}$ such that

$$\int_{\Gamma^-} \boldsymbol{a}.\boldsymbol{n}U^- V ds + \int_{\Gamma^+} \boldsymbol{a}.\boldsymbol{n}UV ds + \iint_\Delta (-\boldsymbol{a}.\nabla V + cV)U dxdy = \iint_\Delta fV dxdy, \quad \forall\ V \in \mathcal{W}_p. \tag{3.5}$$

where U^- is the limit from the $inflow$ element sharing Γ^- , *i.e.*,

$$U^-(x, y) = \lim_{s \to 0^+} U^-(x, y) = \lim_{s \to 0^+} U((x, y) + s\boldsymbol{n}), \quad (x, y) \in \Gamma^-. \tag{3.6}$$

Note that U^- on Γ^- is a given boundary condition while U on Γ^+ is the unknown solution on Γ^+ .

Applying the divergence theorem to (3.5), leads to

$$\int_{\Gamma^-} \boldsymbol{a}.\boldsymbol{n}V(U^- - U) ds + \iint_\Delta (\boldsymbol{a}.\nabla U + cU)V dxdy = \iint_\Delta fV dxdy, \quad \forall\ V \in \mathcal{W}_p. \tag{3.7}$$

The formulation consists of determining $U \in S^{N,p}$ such that

$$a_\Delta(U, V) = F(V), \quad \forall\ V \in \mathcal{W}_p, \tag{3.8}$$

where U^- is given on the $inflow$ boundary Γ^- and

$$a_\Delta(U,V) = \iint_\Delta (\boldsymbol{a}.\nabla U + cU)V\,dxdy - \int_{\Gamma^-} \boldsymbol{a}.\boldsymbol{n}UV\,ds,$$
$$F(V) = \iint_\Delta fV\,dxdy - \int_{\Gamma^-} \boldsymbol{a}.\boldsymbol{n}U^-V\,ds. \tag{3.9}$$

Choosing a basis $\{\varphi_i\}$ for the space $S^{N,p}$ and writing $U = \sum_i c_i\varphi_i$ leads to a algebraic system:

$$A\boldsymbol{C} = \boldsymbol{B},$$

where

$$A_{ij} = \iint_\Delta (\boldsymbol{a}.\nabla\varphi_j + c\varphi_j)\varphi_i dxdy - \int_{\Gamma^-} \boldsymbol{a}.\boldsymbol{n}\varphi_i\varphi_j ds,$$
$$B_i = \iint_\Delta f\varphi_i dxdy - \int_{\Gamma^-} \boldsymbol{a}.\boldsymbol{n}U^-\varphi_i ds.$$

The regularity of the matrix A as well as the uniqueness and existence of the approximation U can be easily proved, see [34].

For the boundary data U^- on Γ^- we use either the exact boundary condition or some suitable interpolant of it

$$U^-(x,y) = \begin{cases} \pi g_0, & (x,y) \in \Gamma_2, \\ \pi g_1, & (x,y) \in \Gamma_1, \end{cases} \tag{3.10}$$

where πw is the one-dimensional $p-$ degree polynomial that interpolates w at the roots of $(p+1)-$ degree Gauss Legendre polynomial and Γ_1, Γ_2 are the $inflow$ boundaries of Δ , see Figure 3.2.

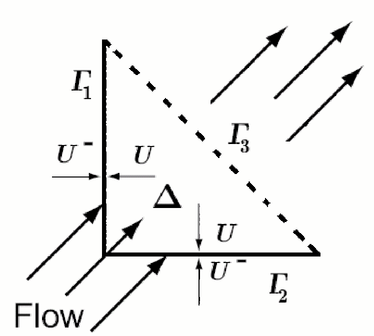

Figure 3.2: Element Δ with $inflow$ boundaries shown with solid lines and $outflow$ boundary with dashed lines.

To obtain the discrete solution $U(x,y)$ in (3.7), we express U as a linear combination of Dubiner basis. We also employ the bilinear mapping defined in (2.40). We note that all the physical domains Ω in this work, are such that the bilinear mapping introduces no error with respect to the geometry. Therefore, using (3.7) we obtain a system of equations to be solved. We solve the algebraic system using Newton's method. Note that since our problem (3.1) is linear, the system of equations to be solved is also linear and thus only one step of Newton's method is required to solve for C.

Once we determine the solution on the first element Δ we proceed to the elements whose $inflow$ boundaries are either on the $inflow$ boundary of Ω or an $outflow$ boundary of Δ and continue this process until the solution is determined in the whole domain. On an element whose $inflow$ boundary is not on the boundary of Ω, U^- is defined as (3.6).

Next we consider the problem (3.5) on an element Δ such that $\Gamma^- \subset \partial\Omega^-$. Let U^- be an approximation of the true solution u on Γ^- and subtract (3.5) from (3.4) with $v = V$ to obtain the DG orthogonality condition for the local finite element discretization error $\epsilon = u - U$

$$\int_{\Gamma^-} \boldsymbol{a}.\boldsymbol{n}\epsilon^- V ds + \int_{\Gamma^+} \boldsymbol{a}.\boldsymbol{n}\epsilon V ds + \iint_{\Delta} (-\boldsymbol{a}.\nabla V + cV)\epsilon dx dy = 0, \qquad \forall\ V \in \mathcal{W}_p. \tag{3.11}$$

For simplicity we consider the DG orthogonality on the right triangle $\Delta = \{(x, y), 0 \leq x, y \leq h, 0 \leq x + y \leq h\}$ where $h = 1/n$ with vertices $(0, 0)$, $(h, 0)$ and $(0, h)$ which after applying the affine mapping (2.40) with $\epsilon(\xi, \eta)$ and $V(\xi, \eta)$ leads to the DG method orthogonality condition on the canonical element

$$\int_{\hat{\Gamma}^-} \boldsymbol{a}.\boldsymbol{n}\hat{\varepsilon}^- \hat{V} d\hat{s} + \int_{\hat{\Gamma}^+} \boldsymbol{a}.\boldsymbol{n}\hat{\epsilon}\hat{V} d\hat{s} - \int_0^1 \int_0^{1-\xi} (\boldsymbol{a}.\nabla\hat{V} - ch\hat{V})\hat{\epsilon} d\eta d\xi = 0, \quad \forall \hat{V} \in \hat{\mathcal{W}}_p. \tag{3.12}$$

We will omit the $\hat{}$ unless we feel it is needed for clarity. Hence the following orthogonality will be used in our analysis

$$\int_{\Gamma^-} \boldsymbol{a}.\boldsymbol{n}\epsilon^- V ds + \int_{\Gamma^+} \boldsymbol{a}.\boldsymbol{n}\epsilon V ds + \iint_{\Delta} (-\boldsymbol{a}.\nabla V + hcV)\epsilon d\xi d\eta = 0, \qquad \forall V \in \mathcal{W}_p. \tag{3.13}$$

In the remainder of the thesis we divide the elements of a triangular mesh into three types as shown in Figure 3.3. Type I, consisting of triangles having one $inflow$ and two $outflow$ edges, Type II, consisting of triangles having two $inflow$ and one $outflow$ edges and Type III, consisting of triangles having one $inflow$, one $outflow$ and one characteristic edge.

To enhance the conditioning of the finite element problem we use Dubiner orthogonal polynomials as shape functions given on the canonical triangle Δ defined by the vertices $A = (0, 0)$, $B = (1, 0)$ and $C = (0, 1))$ as (2.47).

The $(k + l)$-degree polynomials

$$\psi_k^l = P_k^{1,0}(\frac{2\xi}{1-\eta} - 1)(1 - \eta)^k P_l^{2k+2,0}(2\eta - 1),\ \ k, l \geq 0,\ \ k + l \leq p, \tag{3.14a}$$

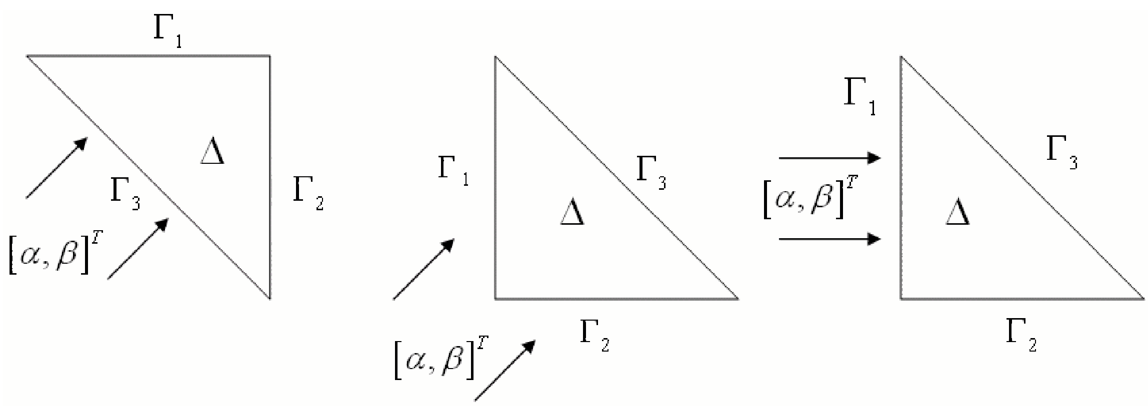

Figure 3.3: Elements of type I (left), II (center) and III (right)

where $P_n^{\alpha,\beta}(x)$ and L_n are the n-th degree Jacobi and Legendre polynomials, respectively, on $[-1,1]$, satisfy the orthogonality condition

$$\int_0^1 \int_0^{1-\eta} (\xi - (1-\eta))\psi_k^l \psi_p^q d\xi d\eta = c_{kp}^{lq}\delta_{kp}\delta_{lq}, \tag{3.14b}$$

and thus provide another basis for $\mathcal{P}_p$.

The finite element spaces $\mathcal{V}_p$ and $\mathcal{U}_p$ are suboptimal, *i.e.*, they contain $p+1$-degree terms that do not contribute to global convergence rate, however, they yield $O(h^{p+2})$ superconvergence rates at some additional interior points which simplifies the *a posteriori* error estimation procedures described later on.

If the exact solution is an analytic function, we can write the local error as a Maclaurin series around $h=0$

$$\epsilon(\xi,\eta) = \sum_{k=0}^{\infty} Q_k(\xi,\eta)h^k, \tag{3.15}$$

where $Q_k \in \mathcal{P}_k$.

Lemma 3.1. *If $Q_k \in \mathcal{P}_k,\ k=0,\cdots,p$ satisfies*

$$\int_{\Gamma^+} \boldsymbol{a}.\boldsymbol{n} Q_0 V ds - \iint_{\Delta} \boldsymbol{a}\cdot\nabla V Q_0 d\xi\ d\eta = 0, \quad \forall\ V \in \mathcal{W}_p, \tag{3.16}$$

and for $1 \le k \le p$,

$$\int_{\Gamma^+} \boldsymbol{a}.\boldsymbol{n} Q_k V ds - \iint_{\Delta} (\boldsymbol{a}\cdot\nabla V Q_k - cVQ_{k-1}) d\xi\ d\eta = 0, \quad \forall\ V \in \mathcal{W}_p. \tag{3.17}$$

Then,

$$Q_k = 0, \quad 0 \le k \le p. \tag{3.18}$$

Proof. We prove this by induction. We first set $V = 1$ in (3.16) shows that $Q_0 = 0$. Now, for $k = 1$, equation (3.17) simplify to

$$\int_{\Gamma^+} \boldsymbol{a}.\boldsymbol{n} Q_1 V ds - \iint_{\Delta} \boldsymbol{a} \cdot \nabla V Q_1 d\xi \; d\eta = 0, \quad \forall V \in \mathcal{W}_p. \tag{3.19}$$

Using Green's formula, equation (3.19) can be written as

$$-\int_{\Gamma^-} \boldsymbol{a}.\boldsymbol{n} Q_1 V ds + \iint_{\Delta} \boldsymbol{a} \cdot \nabla Q_1 V d\xi \; d\eta = 0, \quad \forall V \in \mathcal{W}_p. \tag{3.20}$$

Now, adding (3.19) to (3.20) and we let $V = Q_1$ to obtain

$$-\int_{\Gamma^-} \boldsymbol{a}.\boldsymbol{n} {Q_1}^2 ds + \int_{\Gamma^+} \boldsymbol{a}.\boldsymbol{n} {Q_1}^2 ds = \int_{\Gamma} |\boldsymbol{a}.\boldsymbol{n}| {Q_1}^2 ds = 0. \tag{3.21}$$

From (3.21) we obtain $Q_1 = 0$ on Γ. Combining this with (3.20) for $V = \boldsymbol{a}.\nabla Q_1$ yields $\boldsymbol{a}.\nabla Q_1 = 0$ on Δ which leads to $Q_1 = 0$.

Next, by induction, we assume that $Q_k = 0, \quad \forall k \leq p - 1$ then using equation (3.17) for $k = p$ to obtain

$$\int_{\Gamma^+} \boldsymbol{a}.\boldsymbol{n} Q_p V ds - \iint_{\Delta} \boldsymbol{a} \cdot \nabla V Q_p d\xi \; d\eta = 0, \quad \forall V \in \mathcal{W}_p. \tag{3.22}$$

Again we apply Green's formula to (3.22) we write

$$-\int_{\Gamma^-} \boldsymbol{a}.\boldsymbol{n} Q_p V ds + \iint_{\Delta} \boldsymbol{a} \cdot \nabla Q_p V d\xi \; d\eta = 0, \quad \forall V \in \mathcal{W}_p. \tag{3.23}$$

Now, adding (3.22) to (3.23) and we let $V = Q_p$ we obtain

$$-\int_{\Gamma^-} \boldsymbol{a}.\boldsymbol{n} {Q_p}^2 ds + \int_{\Gamma^+} \boldsymbol{a}.\boldsymbol{n} {Q_p}^2 ds = \int_{\Gamma} |\boldsymbol{a}.\boldsymbol{n}| {Q_p}^2 ds = 0. \tag{3.24}$$

From (3.24) we obtain $Q_p = 0$ on Γ. Combining this with (3.23) for $V = \boldsymbol{a}.\nabla Q_p$ yields $\boldsymbol{a}.\nabla Q_p = 0$ on Δ which leads to $Q_p = 0$. $\square$

Lemma 3.2. *Let $w \in C^\infty(0, h)$ and πw be a $p-$ degree polynomial that interpolates w at shifted roots of Legendre polynomial on $[0, h]$. Then the interpolation error can be written as*

$$w(x(\xi)) - \pi w(x(\xi)) = \sum_{k=p+1}^{\infty} Q_k^-(\xi) h^k, \tag{3.25}$$

where

$$Q_{p+1}^-(\xi) = \frac{w^{(p+1)}(0)}{(p+1)!} \prod_{i=0}^{p} (\xi - \xi_i) = c_{p+1} L_{p+1}(\xi), \tag{3.26}$$

and

$$Q_k^-(\xi) = L_{p+1}(\xi) l_{k-p-1}(\xi), \qquad k > p+1, \tag{3.27}$$

with $l_n(\xi) \in \mathbf{P}_n$, $L_{p+1}(\xi)$ *is the* $(p+1)$*-degree Legendre polynomial and* $x(\xi)$ *is the linear mapping from* $[0,1]$ *to* $[0,h]$.

Proof. By the standard interpolation theory there exists $s(x)$ such that

$$w(x(\xi)) - \pi w(x(\xi)) = \frac{w^{(p+1)}(s(x,h))}{(p+1)!} \prod_{i=0}^{p} (x - x_i), \quad x \in [0,h], \tag{3.28}$$

where $x_i = h\xi_i$ and $\xi_i, i = 0, 1, ..., p$, are the roots of Legendre polynomial L_{p+1} in $[0,1]$. On $[0,1]$ the interpolation error can be written as

$$w(\xi) - \pi w(\xi) = \frac{h^{p+1} w^{(p+1)}(s(x(\xi),h))}{(p+1)!} \prod_{i=0}^{p} (\xi - \xi_i), \quad \xi \in [0,1]. \tag{3.29}$$

The Maclaurin series of $w^{(p+1)}(s(x(\xi),h))$ with respect to h yields

$$w^{(p+1)}(s(x(\xi),h)) = w^{(p+1)}(0) + \sum_{k=1}^{\infty} h^k q_k(\xi), \tag{3.30}$$

where

$$q_k(\xi) = \frac{1}{k!} \frac{d^k w^{(p+1)}(s(x(\xi),h))}{dh^k}|_{h=0}, \quad k > 0, \tag{3.31}$$

is a polynomial of degree k. Combining (3.29),(3.30) and (3.31) completes the proof. □

We recall the following results from Krivodonova and Flaherty [45] which will be needed in our analysis.

Theorem 3.1. *Let* $u \in C^\infty(\triangle)$ *and* $U \in \mathcal{P}_p(\triangle)$ *be the solutions of (3.1) and (3.5), respectively, with* $U^- |_{\Gamma^-} = u$. *If* $\alpha \geq 0$ *and* $\beta \geq 0$ *such that* $\triangle$ *is either a triangle of type II or type III, then the local finite element error can be written as*

$$\epsilon(\xi,\eta) = \sum_{k=p+1}^{\infty} h^k Q_k(\xi,\eta), \tag{3.32}$$

where

$$\iint_{\Delta} Q_{p+1} V d\xi \ d\eta = 0, \qquad \forall \ V \in \mathcal{P}_{p-1}, \tag{3.33}$$

$$\int_{\Gamma^+} \boldsymbol{a}.\boldsymbol{n} Q_{p+1} V ds = 0, \qquad \forall \ V \in \mathcal{P}_p, \tag{3.34}$$

$$\int_{\Gamma^+} \boldsymbol{a}.\boldsymbol{n} Q_k ds = 0, \qquad k \geq p+1, \tag{3.35}$$

$$Q_{p+1}(\xi,\eta) = \sum_{i=0}^{p} c_i^p \varphi_{p-i}^i(\xi,\eta) + \sum_{i=0}^{p+1} c_i^{p+1} \varphi_{p+1-i}^i(\xi,\eta). \tag{3.36}$$

Furthermore, at the outflow boundary of the physical element Δ the local error satisfies

$$\int_{\Gamma^+} \boldsymbol{a}.\boldsymbol{n} \epsilon ds = O(h^{2p+2}). \tag{3.37}$$

Proof. Cf. Krivodonova and Flaherty [45]. □

In order to prove (3.32), we write the Maclaurin series of the local error ϵ with respect to h (u is smooth enough) to obtain (3.15). Substituting the series (3.15) in the DG method orthogonality condition (3.13), using the assumption $U^- |_{\Gamma^-} = u$ and collecting terms having the same powers of h we write

$$\left(\int_{\Gamma^+} \boldsymbol{a}.\boldsymbol{n} Q_0 V ds - \iint_{\Delta} \boldsymbol{a} \cdot \nabla V Q_0 d\xi\, d\eta \right) +$$
$$\sum_{k=1}^{p} h^k \left(\int_{\Gamma^+} \boldsymbol{a}.\boldsymbol{n} Q_k V ds - \iint_{\Delta} (\boldsymbol{a} \cdot \nabla V Q_k - cVQ_{k-1}) d\xi\, d\eta \right) +$$
$$\sum_{k=p+1}^{\infty} h^k \left(\int_{\Gamma^+} \boldsymbol{a} \cdot \boldsymbol{n} Q_k V ds - \iint_{\Delta} (\boldsymbol{a} \cdot \nabla V Q_k - cVQ_{k-1}) d\xi\, d\eta \right) = 0, \quad \forall\, V \in \mathcal{W}_p. \tag{3.38}$$

By Lemma 3.1, (3.38) leads to $Q_k = 0, k = 0, ..., p$, and establishes (3.32). Next, the $O(h^{p+1})$ term leads to

$$\int_{\Gamma^+} \boldsymbol{a} \cdot \boldsymbol{n} Q_{p+1} V ds - \iint_{\Delta} \boldsymbol{a} \cdot \nabla V Q_{p+1} d\xi\, d\eta = 0, \quad \forall V \in \mathcal{W}_p. \tag{3.39}$$

Remark: We also note that (3.32) holds on elements of type I.

In the next section we will investigate the local DG error on elements of type I, II and III using the polynomial spaces $\mathcal{P}_p$, $\mathcal{V}_p$ and $\mathcal{U}_p$.

3.2 Local DG Error Analysis

Now we are ready to state the first new results for the local discretization error using the space $\mathcal{P}_p$ on elements of Type II and III.

Theorem 3.2. *Under the same assumptions as in Theorem 3.1 there exist two constants C_1 and C_2 such that on the outflow edge we have*

$$Q_{p+1}(1-\eta,\eta) = C_1 L_{p+1}(\eta), \tag{3.40a}$$

$$Q_{p+1}(\xi,1-\xi) = C_2 L_{p+1}(\xi). \tag{3.40b}$$

Furthermore,

$$\iint_{\triangle} \frac{\partial Q_{p+1}}{\partial \xi}\xi^i\eta^j d\xi\ d\eta = 0, \qquad i=1,...,p,\ j=0,...,p-1,\ i+j\le p, \tag{3.41}$$

$$\iint_{\triangle} \frac{\partial Q_{p+1}}{\partial \eta}\xi^i\eta^j d\xi\ d\eta = 0, \qquad i=0,...,p-1,\ j=1,...,p,\ i+j\le p, \tag{3.42}$$

and

$$\iint_{\triangle} \boldsymbol{a}.\nabla(1-\xi-\eta)^i Q_{p+1} d\eta d\xi = 0, \quad i=1,...,p. \tag{3.43}$$

Proof. We first note that (3.40) is a direct consequence of (3.34).

In order to prove (3.41), we let

$$I = \iint_{\triangle} \frac{\partial Q_{p+1}(\xi,\eta)}{\partial \xi}\xi^i\eta^j d\xi\ d\eta = \int_0^1 \xi^i\Big(\int_0^{1-\xi} \frac{\partial Q_{p+1}(\xi,\eta)}{\partial \xi}\eta^j\ d\eta\Big)d\xi. \tag{3.44}$$

Differentiating the auxiliary polynomial

$$q(\xi) = \int_0^{1-\xi} Q_{p+1}(\xi,\eta)\eta^j\ d\eta, \tag{3.45}$$

leads to

$$q'(\xi) = -(1-\xi)^j Q_{p+1}(\xi,1-\xi) + \int_0^{1-\xi} \frac{\partial Q_{p+1}(\xi,\eta)}{\partial \xi}\eta^j\ d\eta. \tag{3.46}$$

Combining this with (3.44) yields

$$I = \int_0^1 \xi^i(1-\xi)^j Q_{p+1}(\xi,1-\xi)d\xi + \int_0^1 \xi^i q'(\xi)d\xi. \tag{3.47}$$

First, we note that the orthogonality condition (3.34) for $i+j\le p$ infers that the first term in the right hand side of (3.47) is zero. We integrate the second term in (3.47) by parts and use (3.45) to write

$$I = \xi^i \int_0^{1-\xi} Q_{p+1}(\xi,\eta)\eta^j d\eta\Big|_{\xi=0}^{\xi=1} - i\int_0^1\int_0^{1-\xi} \xi^{i-1}\eta^j Q_{p+1}(\xi,\eta)d\eta d\xi. \tag{3.48}$$

For $i+j \leq p$ and $i>0$, we apply the orthogonality condition (3.33) to establish (3.41). The proof of (3.42) follows the same line of reasoning.

Now we substitute the Maclaurin series of the local error in the DG method orthogonality condition on the canonical element (3.13) with $\mathcal{W}_p = \mathcal{P}_p$ and follow the reasoning of Theorem 3.1 the $O(h^{p+1})$ term to write

$$\int_{\Gamma^+} \boldsymbol{a}\cdot\boldsymbol{n} Q_{p+1} V ds - \iint_{\triangle} \boldsymbol{a}\cdot\nabla V Q_{p+1} d\xi\, d\eta = 0, \quad \forall\, V \in \mathcal{P}_p. \tag{3.49}$$

Since on the canonical element the *outflow* edge is the segment $\eta = 1-\xi,\ 0\leq\xi\leq 1$, (3.49) becomes

$$\int_0^1 \boldsymbol{a}\cdot\boldsymbol{n} Q_{p+1}(1-\eta,\eta)V(1-\eta,\eta)d\eta - \iint_{\triangle} \boldsymbol{a}\cdot\nabla V Q_{p+1} d\xi\, d\eta = 0, \quad \forall\, V \in \mathcal{P}_p. \tag{3.50}$$

Testing against $V=(1-\xi-\eta)^i,\ 1\leq i\leq p$, the first term in (3.50) is zero which establishes (3.43). $\square$

Equation (3.40) infers that the local error is $O(h^{p+2})$ superconvergent at the roots of Legendre polynomial on the *outflow* edge.

In the following theorem we state and prove the same results as in Theorem 3.1 for $U^- = \pi u$, an interpolant of the exact boundary condition at the roots of $p+1$-degree Legendre on the *inflow* edges.

Theorem 3.3. *Under the same assumptions as in Theorem 3.1 with $U^- |_{\Gamma^-} = \pi g$ on each inflow boundary edge the properties (3.32)-(3.37) and (3.40-3.43) still hold.*

Proof. Since the *inflow* term in the orthogonality condition (3.13) is not zero in general, substituting the series (3.32) in the DG orthogonality condition (3.13), using (3.25) and collecting terms having the same powers of h we obtain

$$\sum_{k=p+1}^{\infty} h^k \left(\int_{\Gamma^-} \boldsymbol{a}\cdot\boldsymbol{n} Q_k^- V ds + \int_{\Gamma^+} \boldsymbol{a}\cdot\boldsymbol{n} Q_k V ds - \iint_{\triangle} (\boldsymbol{a}\cdot\nabla V Q_k - cVQ_{k-1}) d\xi\, d\eta \right) = 0,$$
$$\forall\, V \in \mathcal{P}_p. \tag{3.51}$$

A direct application (3.26) reveals that Q_{p+1}^- satisfies

$$\int_{\Gamma^-} \boldsymbol{a}\cdot\boldsymbol{n} Q_{p+1}^- V ds = 0, \qquad \forall\, V \in \mathcal{P}_p.$$

Thus, the $O(h^{p+1})$ term yields

$$\int_{\Gamma^+} \boldsymbol{a}\cdot\boldsymbol{n} Q_{p+1} V ds - \iint_{\Delta} \boldsymbol{a}\cdot\nabla V Q_{p+1} d\xi\, d\eta = 0, \qquad \forall\, V\in\mathcal{P}_p. \tag{3.52}$$

From this point on the proof is the same as for Theorems 3.1 and 3.2. □

Next we consider elements of type II and III using the space $\mathcal{U}_p$.

Noting that $\mathcal{P}_p\subset\mathcal{U}_p$ and $\mathcal{P}_p\subset\mathcal{V}_p$, for $p\ge 1$, we may apply the same proof to establish the results of Theorems 3.1 and 3.2 for $\mathcal{U}_p$ and $\mathcal{V}_p$. However, the DG error in the larger spaces $\mathcal{U}_p$ and $\mathcal{V}_p$ satisfies additional orthogonality conditions on elements of type II and III as stated in the next theorem. We note we only consider $p\ge 1$ since $\mathcal{U}_0=\mathcal{P}_1$.

Theorem 3.4. *Let $p\ge 1$ and $\triangle=\{(\xi,\eta),\ \xi,\eta\ge 0,\ \xi+\eta\le 1\}$ Let $u\in C^\infty(\triangle)$ and $U\in\mathcal{U}_p(\triangle)$ be the solution of (3.1) and (3.5),respectively with $U^-\ |_{\Gamma^-}=u$. If $\alpha\ge 0$ and $\beta\ge 0$ such that $\triangle$ is either of type II or type III, then the local finite element error can be written as in (3.32) where the leading term Q_{p+1}, satisfies the following conditions*

$$\int_0^1 \beta Q_{p+1}(\xi,1-\xi)\xi^{p+1}d\xi + \int_0^1\int_0^{1-\xi} \alpha\xi^{p+1}\frac{\partial Q_{p+1}(\xi,\eta)}{\partial\xi}d\eta d\xi = 0, \tag{3.53}$$

and

$$\int_0^1 \alpha Q_{p+1}(1-\eta,\eta)\eta^{p+1}d\eta + \int_0^1\int_0^{1-\eta} \beta\eta^{p+1}\frac{\partial Q_{p+1}(\xi,\eta)}{\partial\eta}d\xi d\eta = 0. \tag{3.54}$$

If either $\alpha=0,\beta>0$ or $\alpha>0,\beta=0$, i.e., Δ is of type III, then the leading term of the local error is zero on the $outflow$ edge

$$Q_{p+1}(\xi,1-\xi)=0,\quad 0\le\xi\le 1, \tag{3.55}$$

$$Q_{p+1}(1-\eta,\eta)=0,\quad 0\le\eta\le 1. \tag{3.56}$$

Furthermore, if $\alpha>0,\ \beta=0$, then

$$\int_0^1\int_0^{1-\xi} \xi^k Q_{p+1}(\xi,\eta)d\eta d\xi = 0,\quad 0\le k\le p, \tag{3.57}$$

$$\int_0^{1-\xi} \frac{\partial^k Q_{p+1}(\xi,\eta)}{\partial\xi^k}d\eta = 0,\quad k=0,1,\quad 0\le\xi\le 1. \tag{3.58}$$

and

$$\iint_{\triangle} \frac{\partial Q_{p+1}}{\partial\xi}\xi^{p+1}d\eta d\xi = 0. \tag{3.59}$$

Similarly, if $\alpha=0,\ \beta>0$, then

$$\int_0^1\int_0^{1-\eta} \eta^k Q_{p+1}(\xi,\eta)d\xi d\eta = 0,\quad 0\le k\le p, \tag{3.60}$$

$$\int_0^{1-\eta} \frac{\partial^k Q_{p+1}(\xi,\eta)}{\partial \eta^k} d\xi = 0, \quad k = 0,1, \quad 0 \le \eta \le 1, \tag{3.61}$$

and

$$\iint_{\triangle} \frac{\partial Q_{p+1}}{\partial \eta} \eta^{p+1} d\eta d\xi = 0. \tag{3.62}$$

Proof. Inserting the Maclaurin series for the local error (3.32) in the DG method orthogonality condition (3.13) with $U^- \mid_{\Gamma^-} = u$ and $\mathcal{W}_p = \mathcal{U}_p$ the $O(h^{p+1})$ term leads to (3.49) for all $V \in \mathcal{U}_p$.

Testing against $V = \xi^{p+1}$ we obtain

$$\int_0^1 (\alpha+\beta) Q_{p+1}(\xi, 1-\xi)\xi^{p+1} d\xi - \iint_{\triangle} \boldsymbol{a} \cdot \nabla(\xi^{p+1}) Q_{p+1} d\xi \; d\eta = 0, \tag{3.63}$$

which, in turn, can be written as

$$\int_0^1 (\alpha+\beta) Q_{p+1}(\xi, 1-\xi)\xi^{p+1} d\xi - \int_0^1 \left[(\alpha(p+1)\xi^p) \; (\int_0^{1-\xi} Q_{p+1}(\xi,\eta) d\eta)\right] d\xi = 0. \tag{3.64}$$

We consider the polynomials

$$q(\xi) = \int_0^{1-\xi} Q_{p+1}(\xi,\eta) d\eta,$$

and

$$q'(\xi) = -Q_{p+1}(\xi, 1-\xi) + \int_0^{1-\xi} \frac{\partial Q_{p+1}(\xi,\eta)}{\partial \xi} d\eta, \quad 0 \le \xi \le 1. \tag{3.65}$$

We integrate the second term in (3.64) by parts and using (3.65) leads to

$$\int_0^1 (\alpha+\beta) Q_{p+1}(\xi, 1-\xi)\xi^{p+1} d\xi -$$

$$\alpha\xi^{p+1} \int_0^{1-\xi} Q_{p+1}(\xi,\eta) d\eta |_{\xi=0}^{\xi=1} + \int_0^1 \alpha\xi^{p+1} \left(-Q_{p+1}(\xi,1-\xi) + \int_0^{1-\xi} \frac{\partial Q_{p+1}(\xi,\eta)}{\partial \xi} d\eta\right) d\xi = 0. \tag{3.66}$$

Using $q(1) = 0$ we obtain

$$\int_0^1 (\alpha+\beta) Q_{p+1}(\xi, 1-\xi)\xi^{p+1} d\xi - \int_0^1 \alpha\xi^{p+1} Q_{p+1}(\xi,1-\xi) d\xi +$$

$$\int_0^1 \alpha\xi^{p+1} \int_0^{1-\xi} \frac{\partial Q_{p+1}(\xi,\eta)}{\partial \xi} d\eta d\xi = 0. \tag{3.67}$$

Now (3.67) simplifies to

$$\int_0^1 \beta Q_{p+1}(\xi,1-\xi)\xi^{p+1}d\xi + \int_0^1 \alpha\xi^{p+1}\int_0^{1-\xi}\frac{\partial Q_{p+1}(\xi,\eta)}{\partial \xi}d\eta d\xi = 0, \tag{3.68}$$

which establishes (3.53).

In order to prove(3.54) we set $V = \eta^{p+1}$ in (3.50) to obtain

$$\int_0^1 (\alpha+\beta)Q_{p+1}(1-\eta,\eta)\eta^{p+1}d\eta - \iint_{\triangle} \boldsymbol{a}\cdot\nabla(\eta^{p+1})Q_{p+1}d\xi\ d\eta = 0, \tag{3.69}$$

which, in turn, can be written as

$$\int_0^1 (\alpha+\beta)Q_{p+1}(1-\eta,\eta)\eta^{p+1}d\eta - \int_0^1 \left[(\beta(p+1)\eta^p)\ \left(\int_0^{1-\eta} Q_{p+1}(\xi,\eta)d\xi\right)\right] d\eta = 0. \tag{3.70}$$

We consider the polynomials

$$q(\eta) = \int_0^{1-\eta} Q_{p+1}(\xi,\eta)d\xi,$$

and

$$q'(\eta) = -Q_{p+1}(1-\eta,\eta) + \int_0^{1-\eta}\frac{\partial Q_{p+1}(\xi,\eta)}{\partial\eta}d\xi, \quad 0\le\eta\le 1. \tag{3.71}$$

We integrate the second term in (3.70) by parts and using (3.71) leads to

$$\int_0^1 (\alpha+\beta)Q_{p+1}(1-\eta,\eta)\eta^{p+1}d\eta -$$

$$\beta\eta^{p+1}\int_0^{1-\eta} Q_{p+1}(\xi,\eta)d\xi\Big|_{\eta=0}^{\eta=1} + \int_0^1 \beta\eta^{p+1}\left(-Q_{p+1}(1-\eta,\eta) + \int_0^{1-\eta}\frac{\partial Q_{p+1}(\xi,\eta)}{\partial\eta}d\xi\right)d\eta = 0. \tag{3.72}$$

Using $q(1) = 0$ we obtain

$$\int_0^1 (\alpha+\beta)Q_{p+1}(1-\eta,\eta)\eta^{p+1}d\eta - \int_0^1 \beta\eta^{p+1}Q_{p+1}(1-\eta,\eta)d\eta +$$

$$\int_0^1 \beta\eta^{p+1}\int_0^{1-\eta}\frac{\partial Q_{p+1}(\xi,\eta)}{\partial\eta}d\xi d\eta = 0. \tag{3.73}$$

Now (3.73) simplifies to

$$\int_0^1 \alpha Q_{p+1}(1-\eta,\eta)\eta^{p+1}d\eta + \int_0^1 \beta\eta^{p+1}\int_0^{1-\eta}\frac{\partial Q_{p+1}(\xi,\eta)}{\partial\eta}d\xi d\eta = 0, \tag{3.74}$$

which establishes (3.54).

Now consider (3.50) with $\boldsymbol{a} = [\alpha, 0]^t$ leading to

$$\int_0^1 Q_{p+1}(\xi, 1-\xi)V(\xi, 1-\xi)d\xi - \int_0^1 \int_0^{1-\xi} \frac{\partial V}{\partial \xi} Q_{p+1}\ d\eta d\xi = 0, \quad \forall\ V \in \mathcal{U}_p. \tag{3.75}$$

Setting $V = \eta^i,\ 0 \le i \le p+1$ in (3.75) we obtain the orthogonality condition on the $outflow$ edge

$$\int_0^1 Q_{p+1}(\xi, 1-\xi)(1-\xi)^i d\xi = 0, \quad 0 \le i \le p+1. \tag{3.76}$$

Since $Q_{p+1}(\xi, 1-\xi) \in \mathbf{P}_{p+1}$, this leads to $Q_{p+1}(\xi, 1-\xi) = 0$ which establishes (3.55).

We continue the proof by considering (3.50) with $\boldsymbol{a} = [\alpha, 0]^t$ leading to

$$\int_0^1 Q_{p+1}(1-\eta, \eta)V d\eta - \int_0^1 \int_0^{1-\xi} \frac{\partial V}{\partial \xi} Q_{p+1}\ d\eta d\xi = 0, \quad \forall\ V \in \mathcal{U}_p. \tag{3.77}$$

Testing against $V = \eta^i,\ 0 \le i \le p+1$ we obtain the orthogonality condition on the $outflow$ edge

$$\int_0^1 Q_{p+1}(1-\eta, \eta)\eta^i d\eta = 0, \quad 0 \le i \le p+1. \tag{3.78}$$

Since $Q_{p+1}(1-\eta, \eta) \in \mathbf{P}_{p+1}$ we establish (3.56). As a result, (3.77) becomes

$$\int_0^1 \int_0^{1-\xi} \frac{\partial V}{\partial \xi} Q_{p+1}\ d\eta d\xi = 0, \quad \forall\ V \in \mathcal{U}_p. \tag{3.79}$$

Testing against $V = \xi^{k+1}, \quad 0 \le k \le p$, (3.79) yields (3.57).

In order to prove (3.58) for $k = 0$, we consider the $(p+2)$-degree polynomial

$$q(\xi) = \int_0^{1-\xi} Q_{p+1}(\xi, \eta) d\eta,$$

and its derivative

$$q'(\xi) = -Q_{p+1}(\xi, 1-\xi) + \int_0^{1-\xi} \frac{\partial Q_{p+1}(\xi, \eta)}{\partial \xi} d\eta = \int_0^{1-\xi} \frac{\partial Q_{p+1}(\xi, \eta)}{\partial \xi} d\eta, \tag{3.80}$$

where we have used (3.55).
Noting that $q(1) = q'(1) = 0$ we write $q(\xi) = (1-\xi)^2 r(\xi)$, where $r(\xi)$ is a polynomial of degree p. Thus, the orthogonality condition (3.57) yields

$$0 = \int_0^1 \int_0^{1-\xi} (1-\xi)^k Q_{p+1}(\xi, \eta) d\eta d\xi = \int_0^1 (1-\xi)^k \left(\int_0^{1-\xi} Q_{p+1}(\xi, \eta) d\eta \right) d\xi =$$

$$\int_0^1 (1-\xi)^k q(\xi) d\xi, \ 0 \le k \le p. \tag{3.81}$$

Hence, we obtain

$$\int_0^1 (1-\xi)^2 r(\xi)(1-\xi)^k d\xi = 0, \ 0 \le k \le p, \tag{3.82}$$

which infers that $r(\xi)$ is orthogonal to all polynomials in $\mathbf{P}_p$ with respect to the weight function $(1-\xi)^2$. Thus, $q(\xi) = 0$ which completes the proof of (3.58). Finally (3.59) follow immediately from (3.53).

The proof for the case $\boldsymbol{a} = [0, \beta]^t$ is similar. This completes the proof of the theorem. □

In the next theorem we state and prove superconvergence results for elements of type II and III using the space $\mathcal{V}_p$.

Theorem 3.5. *Under the assumption of Theorem 3.1 and using the polynomial space $\mathcal{V}_p$ the leading term in the local DG error on an element of type II or III satisfies*

$$\iint_\triangle \boldsymbol{a}.\nabla Q_{p+1} \xi^i \eta^{p+1-i} d\eta d\xi = 0, \quad i = 1, ..., p. \tag{3.83}$$

Moreover, on an element of type III with $\alpha > 0, \ \beta = 0$

$$\iint_\triangle \frac{\partial Q_{p+1}}{\partial \xi} \xi^i \eta^{p+1-i} d\eta d\xi = 0, \quad i = 1, ..., p, \tag{3.84}$$

and

$$Q_{p+1}(\xi, \eta) = C_1 L_{p+1}(\eta) + C_2 (1-\eta)^{p+1} R_{p+1}(\frac{\xi}{1-\eta}) = C_1 L_{p+1}(\eta) + C_2 \prod_{i=1}^{p+1} (\xi - (1-\eta)\xi_i). \tag{3.85}$$

Similarly, if $\alpha = 0, \ \beta > 0$

$$\iint_\triangle \frac{\partial Q_{p+1}}{\partial \eta} \xi^i \eta^{p+1-i} d\eta d\xi = 0, \quad i = 1, ..., p, \tag{3.86}$$

and

$$Q_{p+1}(\xi, \eta) = C_1 L_{p+1}(\xi) + C_2 (1-\xi)^{p+1} R_{p+1}(\frac{\eta}{1-\xi}) = C_1 L_{p+1}(\xi) + C_2 \prod_{i=1}^{p+1} (\eta - (1-\xi)\xi_i). \tag{3.87}$$

where $\xi_1 < \cdots < \xi_{p+1} = 1$ are the roots of Radau polynomial $L_{p+1} - L_p$ in [0,1].

Proof. Inserting the Maclaurin series for the local error (3.32) in the DG method orthogonality condition (3.13) with $U^- \mid_{\Gamma^-} = u$ and $\mathcal{W}_p = \mathcal{V}_p$ the $O(h^{p+1})$ term leads to

$$\int_{\Gamma^+} \boldsymbol{a}\cdot\boldsymbol{n} Q_{p+1} V ds - \iint_{\triangle} \boldsymbol{a}\cdot\nabla V Q_{p+1} d\xi\, d\eta = 0, \quad \forall\, V \in \mathcal{V}_p. \tag{3.88}$$

On the canonical element the *outflow* edge is the segment $\eta = 1-\xi,\ 0 \le \xi \le 1$, (3.88) becomes

$$\int_0^1 \boldsymbol{a}\cdot\boldsymbol{n} Q_{p+1}(\xi, 1-\xi) V(\xi,1-\xi) d\xi - \iint_{\triangle} \boldsymbol{a}\cdot\nabla V Q_{p+1} d\xi\, d\eta = 0, \quad \forall\, V \in \mathcal{V}_p. \tag{3.89}$$

Testing against $V = \xi^i \eta^{p+1-i},\ 1 \le i \le p$, we obtain

$$\int_0^1 (\alpha+\beta) Q_{p+1}(\xi,1-\xi)\xi^i(1-\xi)^{p+1-i} d\xi - \iint_{\triangle} \boldsymbol{a}\cdot\nabla(\xi^i\eta^{p+1-i}) Q_{p+1} d\xi\, d\eta = 0, \quad 1 \le i \le p, \tag{3.90}$$

which, in turn, can be written as

$$\int_0^1 (\alpha+\beta) Q_{p+1}(\xi,1-\xi)\xi^i(1-\xi)^{p+1-i} d\xi - \int_0^1 [(\alpha i \xi^{i-1}) q(\xi) d\xi -$$

$$\int_0^1 (\beta(p+1-i)\eta^{p-i}) g(\eta) d\eta = 0, \quad 1 \le i \le p, \tag{3.91a}$$

where

$$q(\xi) = \int_0^{1-\xi} \eta^{p+1-i} Q_{p+1}(\xi,\eta) d\eta, \ \text{and}\ g(\eta) = \int_0^{1-\eta} \xi^i Q_{p+1}(\xi,\eta) d\xi. \tag{3.91b}$$

Differentiating $q(\xi)$ and $g(\eta)$ yields

$$q'(\xi) = -(1-\xi)^{p+1-i} Q_{p+1}(\xi,1-\xi) + \int_0^{1-\xi} \eta^{p+1-i} \frac{\partial Q_{p+1}(\xi,\eta)}{\partial \xi} d\eta, \quad 0 \le \xi \le 1, \tag{3.92}$$

and

$$g'(\eta) = -(1-\eta)^i Q_{p+1}(1-\eta,\eta) + \int_0^{1-\eta} \xi^i \frac{\partial Q_{p+1}(\xi,\eta)}{\partial \eta} d\xi, \quad 0 \le \eta \le 1. \tag{3.93}$$

Integrating the second and third terms in (3.91a) by parts and using (3.92) and (3.93) leads to

$$\int_0^1 (\alpha+\beta) Q_{p+1}(\xi,1-\xi)\xi^i(1-\xi)^{p+1-i} d\xi -$$

$$\alpha \xi^i q(\xi)|_{\xi=0}^{\xi=1} + \int_0^1 \alpha \xi^i q'(\xi) d\xi -$$

$$\beta\eta^{p+1-i}g(\eta)|_{\eta=0}^{\eta=1} + \int_0^1 \beta\eta^{p+1-i}g'(\eta)d\eta = 0,\ 1 \le i \le p. \tag{3.94}$$

Using $q(1) = g(1) = 0$ we obtain

$$\int_0^1 (\alpha+\beta)Q_{p+1}(\xi,1-\xi)\xi^i(1-\xi)^{p+1-i}d\xi - \int_0^1 \alpha\xi^i(1-\xi)^{p+1-i}Q_{p+1}(\xi,1-\xi)d\xi +$$
$$\int_0^1 \alpha\xi^i \int_0^{1-\xi} \eta^{p+1-i}\frac{\partial Q_{p+1}(\xi,\eta)}{\partial\xi}d\eta d\xi - \int_0^1 \beta\eta^{p+1-i}(1-\eta)^i Q_{p+1}(1-\eta,\eta)d\eta +$$
$$\int_0^1 \beta\eta^{p+1-i}\int_0^{1-\eta} \xi^i\frac{\partial Q_{p+1}(\xi,\eta)}{\partial\eta}d\xi d\eta = 0, \quad 1 \le i \le p. \tag{3.95}$$

Note that *outflow* boundary terms cancel out and (3.95) becomes

$$\alpha\int_0^1\int_0^{1-\xi} \xi^i\eta^{p+1-i}\frac{\partial Q_{p+1}(\xi,\eta)}{\partial\xi}d\eta d\xi + \beta\int_0^1\int_0^{1-\eta} \xi^i\eta^{p+1-i}\frac{\partial Q_{p+1}(\xi,\eta)}{\partial\eta}d\xi d\eta = 0,$$
$$1 \le i \le p. \tag{3.96}$$

which can be written as

$$\iint_\triangle \boldsymbol{a}.\nabla Q_{p+1}\xi^i\eta^{p+1-i}d\eta d\xi = 0, \quad \forall \quad i = 1,...,p, \tag{3.97}$$

Thus, we establish (3.83).

The conditions (3.84) and (3.86) are obtained from (3.83) by setting $\beta = 0$ and $\alpha = 0$, respectively.

Next, we prove (3.85). Since $\mathcal{P}_p \subset \mathcal{V}_p$, (3.40a) still holds. Thus, one can write the leading term as

$$Q_{p+1}(\xi,\eta) = C_1L_{p+1}(\eta) + (\xi-(1-\eta))q_p(\xi,\eta), \tag{3.98}$$

where $q_p(\xi,\eta) \in \mathcal{P}_p$.

Substituting this into

$$\int_0^1 Q_{p+1}(1-\eta,\eta)V(1-\eta,\eta)d\eta - \int_0^1\int_0^{1-\eta} Q_{p+1}\frac{\partial V}{\partial\xi}d\xi d\eta = 0,\ \forall\ V \in \mathcal{V}_p,$$

we obtain

$$\int_0^1 C_1L_{p+1}(\eta)V(1-\eta,\eta)d\eta - \int_0^1\int_0^{1-\eta}\frac{\partial V}{\partial\xi}\left(C_1L_{p+1}(\eta) + (\xi-(1-\eta))q_p(\xi,\eta)\right)\,d\xi d\eta = 0, \quad \forall\, V \in \mathcal{V}_p. \tag{3.99}$$

After simplification, equation (3.99) can be written as

$$\int_0^1\int_0^{1-\eta}\frac{\partial V}{\partial\xi}(\xi-(1-\eta))q_p(\xi,\eta)\,d\xi d\eta = 0, \quad \forall\ V \in \mathcal{V}_p. \tag{3.100}$$

Testing against $V = \xi^i \eta^j,\ 1 \leq i, j \leq p,\ i + j \leq p + 1$, we obtain

$$\int_0^1 \eta^j \int_0^{1-\eta} (\xi - (1-\eta)) q_p(\xi, \eta) \xi^{i-1} d\xi d\eta = 0,\ i = 1, \cdots, p. \tag{3.101}$$

Using (3.14) we write

$$q(\xi, \eta) = \sum_{i=0}^{p} \sum_{j=0}^{i} c_i^j \psi_i^j. \tag{3.102}$$

By the orthogonality (3.101) we note that $q_p(\xi, \eta) = C_2(1-\eta)^p P_p^{1,0}(\frac{\xi}{1-\eta})$.
Using Radau polynomials (2.45) we obtain

$$(\xi - (1-\eta)) q_p(\xi, \eta) = C_2(1-\eta)^{p+1} R_{p+1}(\frac{\xi}{1-\eta}),$$

which establishes (3.85).
The proof of (3.87) follows the same line of reasoning. □

In the next corollary we state pointwise superconvergence of the DG solution at Legendre points on the *outflow* edge on elements of type II and III.

Corollary 3.1. *Under the assumptions of Theorem 3.1 on a triangle of type II the DG solution in either $\mathcal{P}_p$, $\mathcal{V}_p$ or $\mathcal{U}_p$ is $O(h^{p+2})$ superconvergent at the points*

$$(1-\eta_i, \eta_i), \quad i = 1, \cdots, p+1, \tag{3.103}$$

where $\eta_1 < \cdots < \eta_{p+1}$ are the roots of L_{p+1} shifted to $[0, 1]$.

Proof. Follows directly from Theorem 3.2. □

In the following corollary we state and prove new pointwise superconvergence results at interior points on triangles of type III.

Corollary 3.2. *Under the assumptions of Theorem 3.4 on a triangle of type III with $\alpha > 0$ and $\beta = 0$ and U is the DG solution, the following results hold.*

If $U \in \mathcal{P}_p$ we have $O(h^{p+2})$ superconvergence rates of U at the points

$$(1-\eta_i, \eta_i), \quad i = 1, \cdots, p+1, \tag{3.104}$$

where $\eta_1 < \cdots < \eta_{p+1}$ are the roots of L_{p+1} in $[0, 1]$.

If $U \in \mathcal{V}_p$, then we have $O(h^{p+2})$ superconvergence rates at the points

$$((1-\eta_i)\xi_k, \eta_i), \quad i = 1, \cdots, p+1,\ k = 1, \cdots, p+1, \tag{3.105}$$

where $\xi_1 < \cdots < \xi_{p+1} = 1$, are the roots of Radau polynomial $L_{p+1}(\eta) - L_p(\eta)$ shifted to $[0,1]$ and $\eta_1 < \cdots < \eta_{p+1}$ are the roots of L_{p+1} shifted to $[0,1]$.

Finally, if $U \in \mathcal{U}_p$ we have $O(h^{p+2})$ superconvergence rates at every point on the outflow edge

$$(\xi, 1-\xi), \quad 0 \le \xi \le 1. \tag{3.106}$$

Proof. We note that (3.104) and (3.106) follows directly from Theorems 3.2 and 3.4, respectively. In order to prove (3.105) we note that

$$Q_{p+1} = C_1 L_{p+1}(\eta) + C_2 \prod_{k=1}^{p+1} (\xi - (1-\eta)\xi_k).$$

Thus, on each line $\eta = 1 - \xi/\xi_k$,

$$Q_{p+1} = C_1 L_{p+1}(\eta).$$

□

For elements of type I we consider the DG formulation (3.5) on the right triangle $\triangle$ with vertices $(h,0)$, (h,h) and $(0,h)$ mapped to the reference triangle defined by the vertices $(1,0)$, $(1,1)$ and $(0,1)$.

In the next theorem we state and prove new superconvergence results for elements of type I using the space $\mathcal{U}_p$.

Theorem 3.6. *Let $p \ge 1$ and $\triangle$ denote the reference triangle defined by the vertices $(1,0)$, $(1,1)$ and $(0,1)$. Let $u \in C^\infty(\triangle)$ and $U \in \mathcal{U}_p(\triangle)$ be the solution of (3.1) and (3.5), respectively with $U^- |_{\Gamma^-} = u$. If $\alpha > 0$ and $\beta > 0$, then the local error can be written as (3.32) where the leading term , Q_{p+1}, satisfies the following orthogonality conditions*

$$\int_{\Gamma^+} \boldsymbol{a} \cdot \boldsymbol{n} Q_{p+1} (\beta\xi - \alpha\eta)^i ds = 0, \quad i = 0, ..., p, \tag{3.107}$$

$$\iint_{\triangle} \boldsymbol{a} . \nabla (\xi - 1)^i (\eta - 1)^{j-i} Q_{p+1} d\eta d\xi = 0, \quad 1 \le i < j \le p, \tag{3.108}$$

$$\int_0^1 \beta Q_{p+1}(\xi, 1)(\xi - 1)^i d\xi - i \iint_{\triangle} \alpha (\xi - 1)^{i-1} Q_{p+1} d\xi \, d\eta = 0, \quad i = 1, ..., p+1, \tag{3.109}$$

$$\int_0^1 \alpha Q_{p+1}(1, \eta)(\eta - 1)^i d\eta - i \iint_{\triangle} \beta (\eta - 1)^{i-1} Q_{p+1} d\xi \, d\eta = 0, \quad i = 1, ..., p+1, \tag{3.110}$$

Furthermore,

$$\beta Q_{p+1}(\xi, 1) + \alpha Q_{p+1}(\xi, 1-\xi) + \alpha \int_{1-\xi}^1 \frac{\partial Q_{p+1}(\xi, \eta)}{\partial \xi} d\eta = 0, \quad 0 \le \xi \le 1, \tag{3.111}$$

$$\alpha Q_{p+1}(1,\eta)+\beta Q_{p+1}(1-\eta,\eta)+\beta\int_{1-\eta}^{1}\frac{\partial Q_{p+1}(\xi,\eta)}{\partial\eta}d\xi=0,\quad 0\le\eta\le 1. \tag{3.112}$$

Finally, we have the pointwise superconvergence

$$Q_{p+1}(0,1)=Q_{p+1}(1,0)=0. \tag{3.113}$$

Proof. The DG orthogonality (3.13) can be written as

$$\int_{\Gamma^-}\boldsymbol{a}.\boldsymbol{n}\epsilon^- V ds+\int_{\Gamma^+}\boldsymbol{a}.\boldsymbol{n}\epsilon V ds-\int_0^1\int_{1-\xi}^1(\boldsymbol{a}.\nabla V-chV)\epsilon d\eta d\xi=0,\quad \forall\ V\in\mathcal{U}_p. \tag{3.114}$$

Let us use $U^- |_{\Gamma^-}= u$ and follow the reasoning of Theorem 3.1 we establish (3.32). Substituting (3.32) in (3.114) and collecting the terms with same powers in h, the $O(h^{p+1})$ term yields

$$\int_{\Gamma^+}\boldsymbol{a}\cdot\boldsymbol{n}Q_{p+1}V ds-\iint_{\triangle}\boldsymbol{a}\cdot\nabla V Q_{p+1}d\xi\ d\eta=0,\quad \forall\ V\in\mathcal{U}_p. \tag{3.115}$$

Testing against $V=(\beta\xi-\alpha\eta)^i,\quad i=0,...,p$, we have $\boldsymbol{a}\cdot\nabla V=0$ and establishes (3.107).

Since the two *outflow* edges of $\triangle$ are $\xi=1$ and $\eta=1$, (3.115) may be written as

$$\int_0^1\beta Q_{p+1}(\xi,1)V(\xi,1)d\xi+\int_0^1\alpha Q_{p+1}(1,\eta)V(1,\eta)d\eta-\iint_{\triangle}\boldsymbol{a}\cdot\nabla V Q_{p+1}d\xi\ d\eta=0,$$
$$\forall\ V\in\mathcal{U}_p. \tag{3.116}$$

Testing against $V=(\xi-1)^i(\eta-1)^{j-i},\ 1\le i<j\le p$, the boundary terms in (3.116) are zero which yields (3.108).
Next, we obtain (3.109) and (3.110) from (3.115) by testing against $V=(\xi-1)^i,\quad 1\le i\le p+1$ and $V=(\eta-1)^i,\quad 1\le i\le p+1$, respectively.

Finally, we prove (3.111) by considering the polynomial

$$q(\xi)=\int_{1-\xi}^1 Q_{p+1}(\xi,\eta)d\eta,$$

and

$$q'(\xi)=Q_{p+1}(\xi,1-\xi)+\int_{1-\xi}^1\frac{\partial Q_{p+1}(\xi,\eta)}{\partial\xi}d\eta,\quad 0\le\xi\le 1. \tag{3.117}$$

Testing against $V=(\xi-1)^i,\ 0\le i\le p+1$, in (3.116) we obtain

$$\int_0^1\beta Q_{p+1}(\xi,1)d\xi=0, \tag{3.118}$$

and

$$\int_0^1 \beta Q_{p+1}(\xi,1)(\xi-1)^i d\xi - \int_0^1 \int_{1-\xi}^1 \alpha i(\xi-1)^{i-1} Q_{p+1} d\xi d\eta = 0,\ 1 \le i \le p+1, \tag{3.119}$$

which, in turn, can be written as

$$\int_0^1 \beta Q_{p+1}(\xi,1)(\xi-1)^i d\xi - \int_0^1 \left[(\alpha i(\xi-1)^{i-1}) \ \left(\int_{1-\xi}^1 Q_{p+1}(\xi,\eta) d\eta \right) \right] d\xi =$$

$$\int_0^1 \beta Q_{p+1}(\xi,1)(\xi-1)^i d\xi - \int_0^1 \alpha i(\xi-1)^{i-1} q(\xi) d\xi = 0, \quad 1 \le i \le p+1. \tag{3.120}$$

Integration by parts leads to

$$\int_0^1 \beta Q_{p+1}(\xi,1)(\xi-1)^i d\xi - \alpha(\xi-1)^i q(\xi)|_{\xi=0}^{\xi=1} + \int_0^1 \alpha(\xi-1)^i q'(\xi) d\xi = 0,$$

$$1 \le i \le p+1. \tag{3.121}$$

Noting that the following holds

$$-\alpha(\xi-1)^0 q(\xi)|_{\xi=0}^{\xi=1} + \int_0^1 \alpha(\xi-1)^0 q'(\xi) d\xi = -\alpha q(\xi)|_{\xi=0}^{\xi=1} + \alpha q(\xi)|_{\xi=0}^{\xi=1} = 0,$$

we prove (3.121) for $i = 0$.

Thus,

$$\int_0^1 \beta Q_{p+1}(\xi,1)(\xi-1)^i d\xi - \alpha(\xi-1)^i q(\xi)|_{\xi=0}^{\xi=1} + \int_0^1 \alpha(\xi-1)^i q'(\xi) d\xi = 0, \quad 0 \le i \le p+1. \tag{3.122}$$

Combining $q(0) = 0$, (3.117) and (3.122) we obtain

$$\int_0^1 \beta Q_{p+1}(\xi,1)(\xi-1)^i d\xi + \int_0^1 \alpha(\xi-1)^i \left(Q_{p+1}(\xi,1-\xi) + \int_{1-\xi}^1 \frac{\partial Q_{p+1}(\xi,\eta)}{\partial \xi} d\eta \right) d\xi = 0,$$

$$0 \le i \le p+1, \tag{3.123}$$

which can be written as the orthogonality condition

$$\int_0^1 H_1(\xi)(\xi-1)^i d\xi = 0, \quad i = 0, \cdots, p+1, \tag{3.124}$$

where

$$H_1(\xi) = \beta Q_{p+1}(\xi,1) + \alpha Q_{p+1}(\xi,1-\xi) + \alpha \int_{1-\xi}^1 \frac{\partial Q_{p+1}(\xi,\eta)}{\partial \xi} d\eta, \tag{3.125}$$

is a polynomial of degree $p+1$.
Thus, $H_1(\xi) = 0$ which establishes (3.111).

The proof of (3.112) follow the same line of reasoning by considering the polynomial

$$s(\eta) = \int_{1-\eta}^{1} Q_{p+1}(\xi,\eta)d\xi,$$

and its derivative

$$s'(\eta) = Q_{p+1}(1-\eta,\eta) + \int_{1-\eta}^{1} \frac{\partial Q_{p+1}(\xi,\eta)}{\partial \eta} d\xi, \quad 0 \le \eta \le 1. \tag{3.126}$$

Testing against $V = (\eta-1)^i, \quad 0 \le i \le p+1$ in the orthogonality condition

$$\int_0^1 \beta Q_{p+1}(\xi,1)V(\xi,1)d\xi + \int_0^1 \alpha Q_{p+1}(1,\eta)V(1,\eta)d\eta - \int_0^1 \int_{1-\eta}^1 \boldsymbol{a}\cdot\nabla V Q_{p+1} d\xi d\eta = 0,$$
$$\forall\ V \in \mathcal{U}_p, \tag{3.127}$$

yields

$$\int_0^1 \alpha Q_{p+1}(1,\eta)d\eta = 0, \tag{3.128}$$

and

$$\int_0^1 \alpha Q_{p+1}(1,\eta)(\eta-1)^i d\eta - \int_0^1 (\beta i(\eta-1)^{i-1})s(\eta)d\eta = 0, \quad 1 \le i \le p+1. \tag{3.129}$$

Integration by parts leads to

$$\int_0^1 \alpha Q_{p+1}(1,\eta)(\eta-1)^i d\eta - \beta(\eta-1)^i s(\eta)|_{\eta=0}^{\eta=1} + \int_0^1 \beta(\eta-1)^i s'(\eta)d\eta = 0,$$
$$1 \le i \le p+1. \tag{3.130}$$

Again we note that (3.130) is satisfied for $i=0$ which immediately follows from

$$-\beta(\eta-1)^0 s(\eta)|_{\eta=0}^{\eta=1} + \int_0^1 \beta(\eta-1)^0 s'(\eta)d\eta = -\beta s(\eta)|_{\eta=0}^{\eta=1} + \beta s(\eta)|_{\eta=0}^{\eta=1} = 0.$$

Thus,

$$\int_0^1 \alpha Q_{p+1}(1,\eta)(\eta-1)^i d\eta - \beta(\eta-1)^i s(\eta)|_{\eta=0}^{\eta=1} + \int_0^1 \beta(\eta-1)^i s'(\eta)d\eta = 0,$$
$$1 \le i \le p+1. \tag{3.131}$$

By virtue of the fact that $s(0) = 0$ and (3.126), (3.131) simplifies to

$$\int_0^1 \alpha Q_{p+1}(1,\eta)(\eta-1)^i d\eta + \int_0^1 \beta(\eta-1)^i \left(Q_{p+1}(1-\eta,\eta) + \int_{1-\eta}^1 \frac{\partial Q_{p+1}(\xi,\eta)}{\partial \eta} d\xi \right) d\eta = 0,$$
$$0 \le i \le p+1, \tag{3.132}$$

which can be rewritten as

$$\int_0^1 H_2(\eta)(\eta-1)^i d\eta = 0, \quad i = 0, \cdots, p+1, \tag{3.133}$$

where

$$H_2(\eta) = \alpha Q_{p+1}(1,\eta) + \beta Q_{p+1}(1-\eta,\eta) + \beta \int_{1-\eta}^1 \frac{\partial Q_{p+1}(\xi,\eta)}{\partial \eta} d\xi. \tag{3.134}$$

Thus, $H_2 = 0$, *i.,e.,* (3.112).

We conclude the proof of this Theorem by establishing the pointwise superconvergence (3.113) as

$$0 = H_1(0) = \beta Q_{p+1}(0,1) + \alpha Q_{p+1}(0,1) = (\beta+\alpha) Q_{p+1}(0,1). \tag{3.135}$$

Similarly, $H_2(0) = 0$ leads to

$$H_2(0) = \alpha Q_{p+1}(1,0) + \beta Q_{p+1}(1,0) = (\alpha+\beta) Q_{p+1}(1,0) = 0. \tag{3.136}$$

This completes the proof of the theorem.

We note that (3.107) and (3.108) are also true for $\mathcal{P}_p$ and $\mathcal{V}_p$. □

In the following corollary we show that the DG solution in $\mathcal{U}_1$ on elements of type II and III is $O(h^3)$ superconvergent on curves.

Corollary 3.3. *Under the assumptions of Theorem 3.4 and for $p = 1$ the DG solution on element of type II is $O(h^3)$ superconvergent on the curves*

$$\eta = \frac{2 + s(3-6\xi) + s^2(1-2\xi) - 2\xi - D}{3 + 3s + s^2}, \tag{3.137a}$$

and

$$\eta = \frac{2 + s(3-6\xi) + s^2(1-2\xi) - 2\xi + D}{3 + 3s + s^2}, \tag{3.137b}$$

where $s = \beta/\alpha$ and

$$D = [3\xi(1-2\xi)^2 + (1-\xi)^2 + s^4\xi^2 + s^3(1-6\xi+6\xi^2) + s^2(3-16\xi+25\xi^2)]^{1/2}. \tag{3.137c}$$

Furthermore, on an element of type III the solution is $O(h^3)$ superconvergent on the lines

$$\eta = 1 - \xi \text{ and } \eta = (1-\xi)/3. \tag{3.138}$$

Proof. For $p = 1$ the leading term of the true error can be written as

$$Q_2(\xi,\eta) = c_0 + c_1\xi + c_2\eta + c_3\xi\eta + c_4\xi^2 + c_5\eta^2. \tag{3.139}$$

Applying (3.33), (3.34), (3.53) and (3.54) to obtain

$$Q_2(\xi,\eta) = \frac{c_0}{(\alpha+\beta)^2}[\alpha^2(\xi^2 + (4\eta-2)\xi + 3\eta^2 - 4\eta + 1)+$$

$$\alpha\beta(3\xi^2 + 6(2\eta-1)\xi + 3\eta^2 - 6\eta + 2) + \beta^2(3\xi^2 + 4(\eta-1)\xi + (\eta-1)^2)]. \tag{3.140}$$

We establish (3.137) for type II by solving $Q_2(\xi,\eta) = 0$ for η.

In order to prove (3.138) for type III we first use (3.139) and apply (3.33), (3.34), (3.57) (3.55), *i.e.* $Q_2(\xi, 1-\xi) = 0, \quad 0 \le \xi \le 1$, to obtain

$$Q_2(\xi,\eta) = c_0\left(\xi^2 + (4\eta-2)\xi + 3\eta^2 - 4\eta + 1\right). \tag{3.141}$$

We complete the proof of (3.138) by solving $Q_2(\xi,\eta) = 0$ for η. □

In the following corollary we establish the superconvergence of the DG solution in $\mathcal{U}_p$ on element of type I.

Corollary 3.4. *Under the assumptions of Theorem 3.6 and for $p = 1$ on an element of type I the DG solution is pointwise $O(h^3)$ superconvergent on the two lines*

$$\eta = \frac{(2\alpha+\beta-\alpha\xi)}{2\alpha+\beta} \text{ and } \eta = \frac{(\alpha+2\beta)(1-\xi)}{\beta}. \tag{3.142}$$

Proof. We note that for $p = 1$ the leading term Q_2 of the true error is given by (3.139).

Applying (3.111), (3.112) leads to two polynomials identically zero. By setting their coefficients equal to zero yields a linear system for $c_1, c_2, \cdots, c_6$.
Solving for $c_2, \cdots, c_6$ in terms of c_1 we obtain

$$Q_2(\xi,\eta) =$$

$$c_1\frac{\alpha^2(\xi-1)(\xi+2\eta-2) + \alpha\beta(5 + 2\xi^2 - 7\eta + 2\eta^2 + \xi(6\eta-7)) + \beta^2(\eta-1)(2\xi+\eta-2)}{2\alpha^2 + 5\alpha\beta + 2\beta^2}. \tag{3.143}$$

Finally, we solve $Q_2(\xi,\eta) = 0$ for η to write

$$\eta = \frac{(2\alpha+\beta-\alpha\xi)}{2\alpha+\beta} \text{ and } \eta = \frac{(\alpha+2\beta)(1-\xi)}{\beta}, \tag{3.144}$$

which completes the proof. □

3.3 Nonlinear Convection Reaction Model Problems

In this section we will show that one can extend the above superconvergence results to nonlinear problems of the form

$$\boldsymbol{a}\cdot\nabla u \;+\; \phi(u) = f(x,y), \qquad (x,y)\in\Omega, \tag{3.145}$$

with boundary conditions at the $inflow$ boundary.

The DG method weak formulation consists of determining $U(x,y)\in\mathcal{P}_p$ on an element Δ such that

$$\int_{\Gamma^-}\boldsymbol{a}.\boldsymbol{n}U^-V ds+\int_{\Gamma^+}\boldsymbol{a}.\boldsymbol{n}UV ds-\iint_{\Delta}(\boldsymbol{a}.\nabla VU-\phi(U)V)dxdy=\iint_{\Delta} fV dxdy,\ \forall\ V\in\mathcal{P}_p. \tag{3.146}$$

To obtain the discrete solution $U(x,y)$ in (3.146), we compose U in terms of Dubiner basis. We also employ the bilinear mapping defined in (2.40). Therefore, using (3.146) we obtain a system of equations to be solved. We solve the algebraic system using Newton's method.

In the following theorem we state superconvergence results and local error estimates for nonlinear problems.

Theorem 3.7. *Let $\triangle$ be an element of Type II or III, i.e., having one $outflow$ edge. Let $u\in C^\infty(\triangle)$ and $U\in\mathcal{P}_p(\triangle)$ be the solutions of (3.145) and (3.146),respectively, with $U^-\mid_{\Gamma^-}=u$, then the results of Theorem 3.1 and 3.2 hold.*

Proof. The DG method orthogonality for (3.145) on an element $\triangle=\{(\xi,\eta),0\le\xi,\eta\le h, 0\le\xi+\eta\le h\}$ can be written as

$$\int_{\Gamma^-}\boldsymbol{a}\cdot\boldsymbol{n}\epsilon^-V ds+\int_{\Gamma^+}\boldsymbol{a}\cdot\boldsymbol{n}\epsilon V ds-\int_0^h\int_0^{h-x}[\boldsymbol{a}\cdot\nabla V\epsilon+(\phi(u)-\phi(U))V]dxdy=0,$$
$$\forall\ V\in\mathcal{P}_p. \tag{3.147}$$

Mapping the orthogonality condition (3.147) to the canonical triangle defined by the vertices $(0,0)$, $(1,0)$ and $(0,1)$ yields

$$\int_{\Gamma^-}\boldsymbol{a}\cdot\boldsymbol{n}\epsilon^-V ds+\int_{\Gamma^+}\boldsymbol{a}\cdot\boldsymbol{n}\epsilon V ds-\int_0^1\int_0^{1-\xi}[\boldsymbol{a}\cdot\nabla V\epsilon+h(\phi(u)-\phi(U))V]d\eta\, d\xi=0,$$
$$\forall\ V\in\mathcal{P}_p. \tag{3.148}$$

Assuming ϕ analytic and ϕ'' bounded and using Taylor series of ϕ about u we have

$$\phi(u)-\phi(U)=a(u)\epsilon-\frac{\epsilon^2}{2}\phi''(\bar{u}),\quad a(u)=\phi'(u). \tag{3.149a}$$

The Maclaurin series of $a(u)$ with respect to h yields

$$a(u) = \sum_{k=0}^{\infty} h^k \bar{Q}_k(\xi,\eta), \quad \bar{Q}_k(\xi,\eta) = \frac{\phi^{(k+1)}(u(x(\xi),y(\eta)))}{k!}\frac{d^k u}{dh^k}(x(\xi),y(\eta))|_{h=0} \in \mathcal{P}_k. \quad (3.149\text{b})$$

We note that in order to establish (3.149b) we used the chain rule with $x(\xi) = h\xi$ and $y(\eta) = h\eta$.

Substituting (3.15) and (3.149) in (3.148) and collecting terms having same powers of h lead to

$$\int_{\Gamma^+} \boldsymbol{a}.\boldsymbol{n} Q_0 V ds - \iint_{\Delta} \boldsymbol{a}\cdot\nabla V Q_0 d\xi\ d\eta +$$
$$\sum_{k=1}^{p} h^k \left(\int_{\Gamma^+} \boldsymbol{a}.\boldsymbol{n} Q_k V ds - \iint_{\Delta} [\boldsymbol{a}\cdot\nabla V Q_k + Z_{k-1}V] d\xi\ d\eta\right) +$$
$$\sum_{k=p+1}^{\infty} h^k \left(\int_{\Gamma^+} \boldsymbol{a}\cdot\boldsymbol{n} Q_k V ds - \iint_{\Delta} [\boldsymbol{a}\cdot\nabla V Q_k + Z_{k-1}V] d\xi\ d\eta\right) = 0, \qquad \forall V \in \mathcal{P}_p, \quad (3.150\text{a})$$

where

$$Z_k = \sum_{l=0}^{k} \bar{Q}_l Q_{k-l}. \quad (3.150\text{b})$$

Applying Lemma 3.1, the $O(1)$ term yields $Q_0 = 0$. By induction we prove that $Q_k = 0,\ k = 0,1,\ldots,p$. We note that the term in (3.149a) involving ϵ^2 is higher order and does not contribute to our leading terms.

Following the same lines of reasoning used to prove (3.40a) we establish the same result for nonlinear problems. □

The results of Theorems 3.4-3.6 also hold for the nonlinear problem (3.145).

In the next section, we investigate the superconvergence of DG solutions for nonlinear hyperbolic problems.

3.4 Nonlinear Conservation Laws

We consider the nonlinear hyperbolic scalar problems

$$\nabla\cdot\mathbf{F}(u) = h(u)_x + g(u)_y = f(x,y), \quad (x,y) \in \Omega = [0,1]^2 \quad (3.151)$$

with boundary conditions

$$u(x,0) = h_0(x), \quad u(0,y) = h_1(y), \quad (3.152)$$

In our analysis we assume $\mathbf{F} : \mathbf{R} \to \mathbf{R}^2$, $u : \mathbf{R}^2 \to \mathbf{R}$, f, h_0 and h_1 to be analytic functions. We also assume that $h'(u) > 0$ and $g'(u) > 0$, so that edges 1 and 2 of our element Δ shown in Figure 3.2 will be *inflow* edges. The *inflow*, *outflow* and characteristic boundaries for nonlinear model are defined as follows

$\partial\Omega^- = \{(x, y) \in \partial\Omega \mid \frac{d\mathbf{F}}{du} \cdot \boldsymbol{n} = [h'(u), g'(u)].\boldsymbol{n} < 0\}$, is the *inflow* boundary,
$\partial\Omega^+ = \{(x, y) \in \partial\Omega \mid \frac{d\mathbf{F}}{du} \cdot \boldsymbol{n} = [h'(u), g'(u)].\boldsymbol{n} > 0\}$, is the *outflow* boundary and
$\partial\Omega^0 = \{(x, y) \in \partial\Omega \mid \frac{d\mathbf{F}}{du} \cdot \boldsymbol{n} = [h'(u), g'(u)].\boldsymbol{n} = 0\}$, is the characteristic boundary.

where the boundary of Ω, $\partial\Omega = \partial\Omega^- \cup \partial\Omega^+ \cup \partial\Omega^0$ and $\boldsymbol{n}$ is the outward unit normal to $\partial\Omega$.

In order to obtain the weak DG formulation, we partition the domain Ω into a regular mesh having N triangular elements $\Delta_j, j = 1, ..., N$, of diameter $h > 0$, and assume, for simplicity, that this can be done without error.

Let us multiply (3.151) by a test function v, integrate over an arbitrary element Δ, and apply Green's theorem to write

$$\int_{\Gamma^-} \boldsymbol{n} \cdot \mathbf{F}(u) v ds + \int_{\Gamma^+} \boldsymbol{n} \cdot \mathbf{F}(u) v ds - \iint_{\Delta} \mathbf{F}(u) \cdot \nabla v dxdy = \iint_{\Delta} f(x, y) v dxdy. \quad (3.153)$$

where Γ^+ and Γ^-, respectively, denote the *outflow* boundary and *inflow* boundaries of Δ.

The discrete DG formulation consists of determining $U \in S^{N,p}$ such that

$$\int_{\Gamma^-} \boldsymbol{n} \cdot \mathbf{F}(U^-) V ds + \int_{\Gamma^+} \boldsymbol{n} \cdot \mathbf{F}(U) V ds - \iint_{\Delta} \mathbf{F}(U) \cdot \nabla V dxdy = \iint_{\Delta} f V dxdy, \quad \forall\, V \in \mathcal{W}_p. \quad (3.154)$$

Applying the divergence theorem to the third term in (3.154), leads to the following discrete weak form: Find $U(x, y) \in \mathcal{W}_p$ on an element Δ such that

$$\int_{\Gamma^-} \boldsymbol{n}.[h(U) - h(U^-), g(U) - g(U^-)] V ds - \iint_{\Delta} (h(U)_x + g(U)_y - f) V dxdy = 0, \ \forall\, V \in \mathcal{W}_p. \quad (3.155)$$

For the boundary data U^- on Γ^- we use either the exact boundary condition or their interpolants defined

$$U^-(x, y) = \begin{cases} \pi h_0, & (x, y) \in \Gamma_2, \\ \pi h_1, & (x, y) \in \Gamma_1, \end{cases} \quad (3.156)$$

where Γ_1, Γ_2 are the *inflow* boundaries of Δ , see Figure 3.2.

Computationally, to determine *inflow* sides of Δ we let $\boldsymbol{n}$ be the unit outward normal to Γ , then for each *inflow* edge where U^- exists, we check

$\Gamma^- = \{(x,y) \in \partial\Delta \mid [h'(U^-), g'(U^-)].\boldsymbol{n}|_{(x^*,y^*)} < 0\}$, *inflow* boundary,
$\Gamma^+ = \{(x,y) \in \partial\Delta \mid [h'(U^-), g'(U^-)].\boldsymbol{n}|_{(x^*,y^*)} > 0\}$, *outflow* boundary,
$\Gamma^0 = \{(x,y) \in \partial\Delta \mid [h'(U^-), g'(U^-)].\boldsymbol{n}|_{(x^*,y^*)} = 0\}$, characteristic boundary.

where (x^*, y^*) is the midpoint of the edge in question. To obtain the discrete solution $U(x,y)$ in (3.155), we compose U in terms of Dubiner basis. We also employ the bilinear mapping defined in (2.40). Therefore, using (3.155) we obtain a system of equations to be solved. In order to solve this system we use Newton's method. For the initial guess, we solve the following linearized system of equations

$$\int_{\Gamma^-} \boldsymbol{n}.[\alpha,\beta](U-U^-)V ds - \iint_{\Delta} (\alpha U_x + \beta U_y - f)V dxdy = 0, \ \forall\ V \in \mathcal{W}_p. \tag{3.157a}$$

where

$$\alpha = h'(U^*) \text{ and } \beta = g'(U^*), \tag{3.157b}$$

and

$$U^* = \frac{U_1^*(x_1^*, y_1^*) + U_2^*(x_2^*, y_2^*)}{2}, \tag{3.157c}$$

with $U_i^*(x_i^*, y_i^*)$ being U^- evaluated at the midpoint of edge i. Once we solve (3.157a) for U we use it to start Newton's method and solve (3.155). Having found our approximate solution on element Δ we move to the next element in the direction of the characteristic flow and repeat the process until we go over all the elements.

Note in (3.157a) the trial and test functions are represented as a linear combination of Dubiner polynomials which leads to better conditioned algebraic systems. The systems given above are solved using Gaussian elimination, see Kincaid and Cheney [43] for more details.

Next we consider the problem (3.154) on an element Δ such that $\Gamma^- \subset \partial\Omega^-$. Let U^- be an approximation of the true solution u on Γ^- and subtract (3.154) from (3.153) with $v = V$ to obtain the DG orthogonality condition for the local error

$$\int_{\Gamma^-} \boldsymbol{n} \cdot (\mathbf{F}(U^-) - \mathbf{F}(u))V ds + \int_{\Gamma^+} \boldsymbol{n} \cdot (\mathbf{F}(U) - \mathbf{F}(u))V ds -$$
$$\iint_{\Delta} (\mathbf{F}(U) - \mathbf{F}(u)) \cdot \nabla V dxdy = 0, \qquad \forall\ V \in \mathcal{W}_p. \tag{3.158}$$

We map a physical triangle Δ having vertices $(x_i, y_i),\ i = 1,2,3$ into the canonical triangle $(0,0)$, $(1,0)$ and $(0,1)$ by the standard affine mapping defined in (2.40). For simplicity we consider the DG orthogonality on the right triangle with vertices $(0,0)$, $(h,0)$ and $(0,h)$ which after applying the affine mapping with $U^-(\xi,\eta)$, $u(\xi,\eta)$ and $V(\xi,\eta)$ leads to

$$\int_{\Gamma^-} \boldsymbol{n} \cdot (\mathbf{F}(U^-) - \mathbf{F}(u))V ds + \int_{\Gamma^+} \boldsymbol{n} \cdot (\mathbf{F}(U) - \mathbf{F}(u))V ds -$$

$$\iint_{\Delta} (\mathbf{F}(U) - \mathbf{F}(u)) \cdot \nabla V d\xi d\eta = 0, \quad \forall\, V \in \mathcal{W}_p. \tag{3.159}$$

We show that the discontinuous finite element solution of (3.151) is $O(h^{p+2})$ superconvergent at the Legendre points on the $outflow$ edge for triangles having one $outflow$ edge. For triangles having two $outflow$ edges the finite element error is $O(h^{p+2})$ superconvergent at the end points of the $inflow$ edge. The flux is $O(h^{2p+2})$ superconvergent on average at the $outflow$ boundary of the first $inflow$ element.

Assuming $\frac{d\mathbf{F}}{du}(u(0,0)) = [\alpha, \beta]^t$, with $\alpha, \beta > 0$, one can prove that for h small enough the $inflow$ boundary of Δ is $\Gamma^- = \Gamma_1 \cup \Gamma_2$ where $\Gamma_1 = \{(x, 0), 0 < x < h\}$ and $\Gamma_2 = \{(0, y), 0 < y < h\}$. The $outflow$ boundary $\Gamma^+ = \Gamma_3$ with $\Gamma_3 = \{(x, y),\ 0 < x, y < h\ \ 0 < y < h - x\}$. To simplify the global error analysis, we also assume that each component of $\frac{d\mathbf{F}}{du}(u(x, y))$ is positive on Ω.

Now we are ready to state the main result for nonlinear conservation laws.

Theorem 3.8. *Let $u \in C^\infty(\triangle)$ and $U \in \mathcal{P}_p(\triangle)$ be the solutions of (3.151) and (3.154), respectively, with $U^- |_{\Gamma^-}= u$. If $\triangle$ is either a triangle of type II or type III. Then the local finite element error*

$$\epsilon = U - u \tag{3.160}$$

can be written as

$$\epsilon(\xi, \eta) = \sum_{k=p+1}^{\infty} h^k Q_k(\xi, \eta), \tag{3.161}$$

where

$$Q_{p+1}(1 - \eta, \eta) = C_1 L_{p+1}(\eta), \quad Q_{p+1}(\xi, 1 - \xi) = C_2 L_{p+1}(\xi). \tag{3.162}$$

Furthermore, at the $outflow$ boundary of the physical element Δ

$$\int_{\Gamma^+} \boldsymbol{n} \cdot (\mathbf{F}(u) - \mathbf{F}(U))\ ds = O(h^{2p+2}). \tag{3.163}$$

Proof. The proof is established using the DG orthogonality condition (3.159).

First we write the Taylor series of $\mathbf{F}$ about u to obtain

$$\mathbf{F}(U) - \mathbf{F}(u) = \sum_{k=1}^{\infty} \frac{\mathbf{F}^{(k)}(u)}{k!} (U - u)^k. \tag{3.164}$$

Assuming $U^- = u$ then (3.159) simplifies to

$$\int_{\Gamma^+} \boldsymbol{n} \cdot (\mathbf{F}(U) - \mathbf{F}(u)) V ds - \iint_{\Delta} (\mathbf{F}(U) - \mathbf{F}(u)) \cdot \nabla V d\xi d\eta = 0, \quad \forall\, V \in \mathcal{W}_p. \tag{3.165}$$

The Maclaurin series of $U-u$ and $\mathbf{F}^{(k)}(u)$ with respect to h can be written as

$$U-u=\sum_{l=0}^{\infty} Q_l h^l, \tag{3.166a}$$

where

$$Q_l(\xi,\eta)=\frac{1}{l!}\frac{d^l(U-u)}{dh^l}|_{h=0}. \tag{3.166b}$$

We also have

$$\mathbf{F}^{(k)}(u)=\sum_{l=0}^{\infty} \boldsymbol{\Phi}_l^{[k]} h^l, \tag{3.167a}$$

where

$$\boldsymbol{\Phi}_l^{[k]}(\xi,\eta)=\frac{1}{l!}\frac{d^l\mathbf{F}^{(k)}(u)}{dh^l}|_{h=0}. \tag{3.167b}$$

Combining (3.164), (3.166) and (3.167) yields

$$\mathbf{F}(U)-\mathbf{F}(u)=\sum_{k=0}^{\infty} \mathbf{W}_k h^k, \tag{3.168}$$

where $\mathbf{W}_k \in \mathcal{P}_k \times \mathcal{P}_k$.

Substituting (3.168) in (3.165) and collecting terms having the same powers of h lead to

$$\sum_{k=0}^{p} h^k \left(\int_{\Gamma^+} \boldsymbol{n}\cdot\mathbf{W}_k V ds - \iint_{\Delta} \mathbf{W}_k\cdot\nabla V d\xi d\eta\right)+$$

$$\sum_{k=p+1}^{\infty} h^k \left(\int_{\Gamma^+} \boldsymbol{n}\cdot\mathbf{W}_k V ds - \iint_{\Delta} \mathbf{W}_k\cdot\nabla V d\xi d\eta\right)=0, \quad \forall V\in\mathcal{W}_p, \tag{3.169}$$

The $O(1)$ term in (3.169) with $V=1$ yields

$$\mathbf{W}_0=Q_0\left(\sum_{l=0}^{\infty}\frac{\boldsymbol{\Phi}_0^{[l+1]}Q_0^l}{(l+1)!}\right)=0, \tag{3.170}$$

which in turn leads to $Q_0=0$. We note that, for instance, for $\mathbf{F}(u)=[u^2/2,u]^t$ there exists $Q_0\neq 0$ solution of (3.170) which corresponds to a *non physical* DG solution with $\epsilon=O(1)$. Here, we will not consider such *non physical* solutions.

By induction the $O(h^k),\ k<p+1$ leads to

$$\int_{\Gamma^+} \boldsymbol{n}\cdot\boldsymbol{\Phi}_0^{[1]} Q_k V ds - \iint_{\Delta} Q_k\boldsymbol{\Phi}_0^{[1]}\cdot\nabla V d\xi d\eta=0,\ \forall V\in\mathcal{W}_p. \tag{3.171}$$

Applying Lemma 3.1 we establish that $Q_k=0,\ k=1,2,\ldots p$.

The $O(h^{p+1})$ term in (3.169) yields

$$\int_{\Gamma^+} \boldsymbol{n} \cdot \boldsymbol{\Phi}_0^{[1]} Q_{p+1} V ds - \iint_{\triangle} Q_{p+1} \boldsymbol{\Phi}_0^{[1]} \cdot \nabla V d\xi d\eta = 0, \ \forall V \in \mathcal{W}_p. \tag{3.172}$$

Following the same line of reasoning as in Theorems 3.1 and 3.2, we establish (3.161)-(3.163). □

In the next theorem we state and prove new superconvergence results for elements of type I using the space $\mathcal{U}_p$.

Theorem 3.9. *Let $p \geq 1$ and $\triangle$ denote the reference triangle defined by the vertices $(1,0)$, $(1,1)$ and $(0,1)$. Let $u \in C^\infty(\triangle)$ and $U \in \mathcal{U}_p(\triangle)$ be the solution of (3.151) and (3.154), respectively with $U^- |_{\Gamma^-} = u$. Then the local error can be written as (3.161) where the leading term , Q_{p+1}, satisfies*

$$Q_{p+1}(0,1) = Q_{p+1}(1,0) = 0. \tag{3.173}$$

Proof. Following the same line of reasoning as in Theorem 3.8, we show that the leading therm of the local error satisfies

$$\int_{\Gamma^+} \boldsymbol{n} \cdot \boldsymbol{\Phi}_0^{[1]} Q_{p+1} V ds - \iint_{\triangle} Q_{p+1} \boldsymbol{\Phi}_0^{[1]} \cdot \nabla V d\xi d\eta = 0, \ \forall V \in \mathcal{W}_p. \tag{3.174}$$

Following the same line of reasoning as in Theorem 3.6, we establish (3.173). □

We have seen computational evidence suggesting that the leading term in the true local error for these nonlinear conservation laws satisfy the same results as in linear conservation laws.

3.5 Local Superconvergence Points

In this section we summarize our pointwise superconvergence results of the local discretization error on triangles of type I, II and III using the three polynomial spaces $\mathcal{P}_p$, $\mathcal{U}_p$ and $\mathcal{V}_p$.

1. On elements of type I we discovered that

   (a) if $U \in \mathcal{P}_p$ or $U \in \mathcal{V}_p$, then U has no superconvergence points. We computed the leading term Q_{p+1} of the true DG error using *Mathematica* for several problems and solutions and discovered that the points and/or curves where the leading term $Q_{p+1}(\xi, \eta) = 0$ vary with each solution and problem.

(b) if $U \in \mathcal{U}_p$, then U is $O(h^{p+2})$ superconvergent at the vertices of the $inflow$ edge for all p which are solution and problem independent. Furthermore, from corollary 3.4 the DG solution for $p = 1$ is superconvergent at every point on the two lines

$$y = \frac{(2\alpha + \beta - \alpha x)}{(2\alpha + \beta)} \text{ and } y = \frac{(\alpha + 2\beta)(1 - x)}{\beta}, \tag{3.175}$$

as shown in Figure 3.4 for $[\alpha, \beta] = [1, 1]$.
If $p > 1$, then the DG solution in $\mathcal{U}_p$ is $O(h^{p+2})$ superconvergent at interior points which depend on α and β. For instance, we show the superconvergence points in Figure 3.4 with coordinates presented in Table 3.1 for $p = 2$ and $[\alpha, \beta] = [1, 1]$. These superconvergence points are obtained from Theorem 3.6. Moreover, in Theorem 3.6 we proved the superconvergence of a functional.

2. On elements of type II we observe that the DG solution in either $\mathcal{P}_p$, $\mathcal{V}_p$, or $\mathcal{U}_p$ is $O(h^{p+2})$ superconvergent at the shifted roots of $(p+1)$-degree Legendre polynomial on the $outflow$ edge as shown in Figures 3.5, 3.6 and 3.7. Furthermore,

(a) If $U \in \mathcal{P}_p$, there are no interior superconvergence points. The proof is the same as for case 1(a).

(b) If $U \in \mathcal{V}_p$, then U is $O(h^{p+2})$ superconvergent at interior points which are independent of the solution but they dependent on mesh orientation and problem parameters α and β. We display these points in Figure 3.6 for $p = 1, 2, 3$, and $[\alpha, \beta] = [1, 1]$. If $p = 1$, U has the unique interior superconvergence point given by

$$x = \frac{9\alpha^2 + 12\alpha\beta + 27\beta^2 - (\alpha - 3\beta)\sqrt{3(9\alpha^2 + 14\alpha\beta + 9\beta^2)}}{6(9\alpha^2 + 2\alpha\beta + 9\beta^2)}, \tag{3.176a}$$

$$y = \frac{9\alpha^2 + 12\alpha\beta + 27\beta^2 - (\alpha - 3\beta)\sqrt{3(9\alpha^2 + 14\alpha\beta + 9\beta^2)}}{6(9\alpha^2 + 2\alpha\beta + 9\beta^2)}. \tag{3.176b}$$

This is obtained by combining (3.139), (3.83), (3.33) and (3.34) to determine Q_2 and solving $Q_2(\xi, \eta) = 0$.
For $p = 2$ and $p = 3$ the interior superconvergence points are shown in Table 3.2 for $[\alpha, \beta] = [1, 1]$. These results are obtained from Theorem 3.5.

(c) If $U \in \mathcal{U}_p$, then U is $O(h^{p+2})$ superconvergent at the following interior points:
If $p = 1$, Corollary 3.3 shows that the DG solution is $O(h^3)$ superconvergent on the curves

$$y = \frac{2 + s(3 - 6x) + s^2(1 - 2x) - 2x - D}{3 + 3s + s^2}, \tag{3.177a}$$

and

$$y = \frac{2 + s(3 - 6x) + s^2(1 - 2x) - 2x + D}{3 + 3s + s^2}, \tag{3.177b}$$

where $s = \beta/\alpha$ and

$$D = [3x(1-2x)^2+(1-x)^2+s^4x^2+s^3(1-6x+6x^2)+s^2(3-16x+25x^2)]^{1/2}. \quad (3.177c)$$

If $p > 1$, then there are interior superconvergence points which depend on α and β but solution independent. They are shown in Figure 3.7 with their coordinates in Table 3.3 for $[\alpha, \beta] = [1, 1]$ and $p = 2, 3$. These points are computed by applying Theorem 3.4.

3. On elements of type III, with $\alpha > 0,\ \beta = 0$, the DG solution in $\mathcal{P}_p$, $\mathcal{V}_p$ or $\mathcal{U}_p$ is $O(h^{p+2})$ superconvergent at the roots of $(p+1)$-degree Legendre polynomial on the *outflow* edge. Furthermore,

   (a) If $U \in \mathcal{P}_p$, there are no interior superconvergence points. The proof is the same as for case 1(a).

   (b) If $U \in \mathcal{V}_p$, then U is again $O(h^{p+2})$ superconvergent at the interior superconvergence points shown in Figure 3.8, Table 3.4 and given by (3.105).

   (c) If $U \in \mathcal{U}_p$, then U is $O(h^{p+2})$ superconvergent at every point on the *outflow* edge $\eta = 1 - \xi$ for all p. Furthermore, for $p = 1$ the DG solution is superconvergent on the line $\eta = (1 - \xi)/3$ as shown in Corollary 3.3 while for $p > 1$ the DG solution is superconvergent a the interior points shown in Figure 3.9 and Table 3.5 (These points are solution and problem independent). These results are obtained from Theorem 3.4.

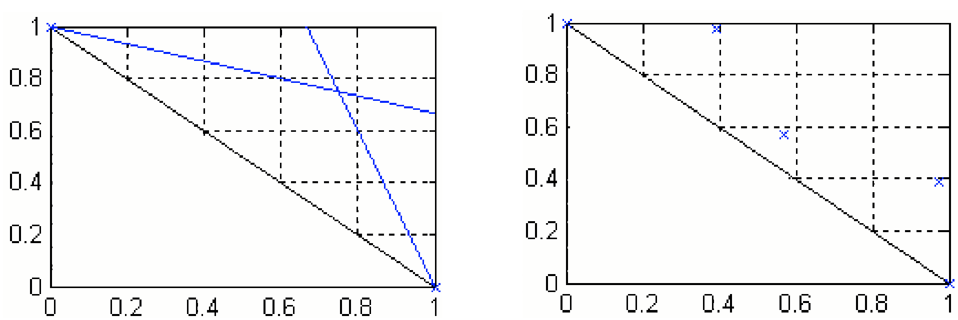

Figure 3.4: Superconvergence points (marked by $\times$) and the lines given by (3.175) on a triangle of type I, where $\alpha > 0$, and $\beta > 0$, $U \in \mathcal{U}_p$ with $p = 1$ (left) and superconvergence points for $p = 2$ (right).

3.6 Global Error Analysis

Superconvergence of local errors is not sufficient to explain the success of the global *a posteriori* error estimates. However, the global solution flux converges at an $O(h^{2p+1})$ rate on

Table 3.1: Interior Superconvergence points on a triangle of type I for $U \in \mathcal{U}_p$ and $[\alpha, \beta] = [1, 1]$ and $p = 2$.

Xcoordinate	Ycoordinate
0.5692303829166225	0.5692303829166225
0.3907670801166887	0.9728692835196749
0.9728692835196749	0.3907670801166887

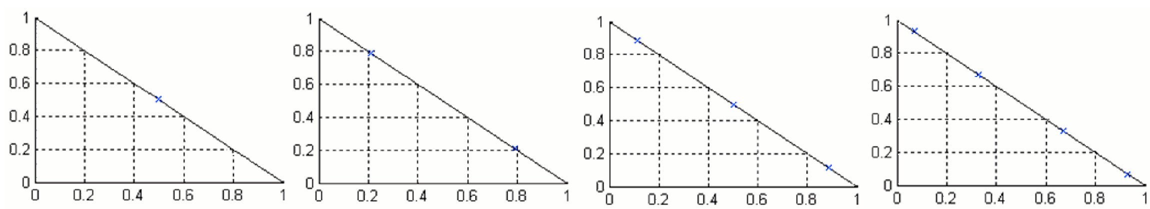

Figure 3.5: Legendre superconvergence points (marked by $\times$) on a triangle of type II, $\alpha > 0$ and $\beta > 0$, using $\mathcal{P}_p$, $p = 0$ to 3 (left to right).

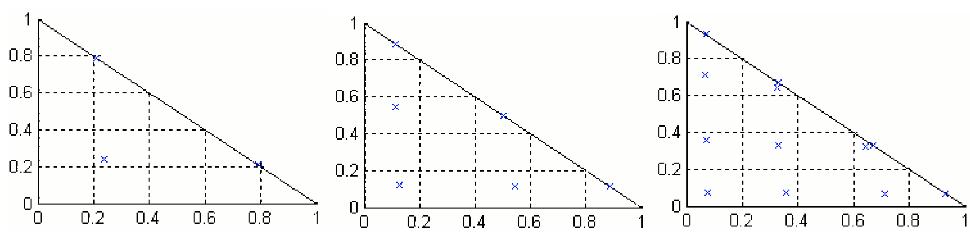

Figure 3.6: Superconvergence points (marked by $\times$) on a triangle of type II, $\alpha > 0$ and $\beta > 0$, using $\mathcal{V}_p$, $p = 1, 2, 3$ (left to right).

Table 3.2: Superconvergence points (marked by $\times$) on a triangle of type II, $\alpha = \beta = 1$, and using $\mathcal{V}_p$, $p = 2, 3$.

	Xcoordinate	Ycoordinate
p=2	$\frac{1}{8}$	$\frac{1}{8}$
	0.1127034090707391	0.544151040560637
	0.544151040560637	0.1127034090707391
p=3	0.0758804897126190	0.0758804897126190
	0.3300667726231823	0.3300667726231823
	0.7133184949549211	0.0669650780843944
	0.3583250921228201	0.0706589671798493
	0.0706589671798493	0.3583250921228201
	0.6406971959045646	0.3236917369067776
	0.3236917369067776	0.6406971959045646
	0.0669650780843944	0.7133184949549211

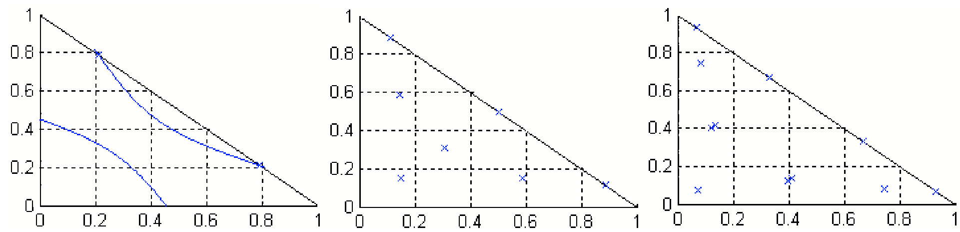

Figure 3.7: Superconvergence points (marked by $\times$) on a triangle of type II, $\alpha > 0$ and $\beta > 0$ using $\mathcal{U}_p$, $p = 1, 2, 3$ (left to right). For $p = 1$ we show two curves of superconvergence points given by (3.177).

Table 3.3: Superconvergence points (marked by $\times$) on a triangle of type II, $\alpha = \beta = 1$ using $\mathcal{U}_p$, $p = 2, 3$.

	Xcoordinate	Ycoordinate
$p = 2$	0.1485431451105056	0.1485431451105056
	0.3060023094349489	0.3060023094349489
	0.14624725188345022	0.587313694956177
	0.587313694956177	0.14624725188345022
$p = 3$	0.07199007958158901	0.07199007958158901
	0.11927967790895	0.39960713026123185
	0.13508195250796606	0.4131816156997246
	0.08240733435311685	0.7452689877115892
	0.3996071302612318	0.11927967790894983
	0.4131816156997246	0.135081952507966
	0.7452689877115892	0.08240733435311683

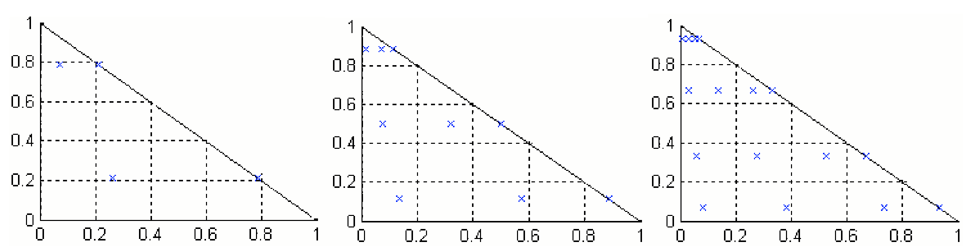

Figure 3.8: Superconvergence points (marked by $\times$) on triangle of type III, $\alpha > 0$ and $\beta = 0$, using $\mathcal{V}_p$, $p = 1$ (left), $p = 2$ (center) and $p = 3$ (right).

Table 3.4: Interior superconvergence points on a triangle of type III, $\alpha > 0$ and $\beta = 0$, using $\mathcal{V}_p$, $p = 1, 2, 3$.

	Xcoordinate	Ycoordinate
$p = 1$	$\frac{3-\sqrt{3}}{18}$	$\frac{3+\sqrt{3}}{6}$
	$\frac{3+\sqrt{3}}{18}$	$\frac{3-\sqrt{3}}{6}$
$p = 2$	$\frac{4-\sqrt{6}}{20}$	$\frac{1}{2}$
	$\frac{4+\sqrt{6}}{20}$	$\frac{1}{2}$
	0.13757651690408637	$\frac{5-\sqrt{15}}{10}$
	0.572262150792507	$\frac{5-\sqrt{15}}{10}$
	0.017474508817583268	$\frac{5+\sqrt{15}}{10}$
	0.0726868234858378	$\frac{5+\sqrt{15}}{10}$
$p = 3$	0.059353093218443065	$\frac{35-\sqrt{35(15-2\sqrt{30})}}{70}$
	0.2743389181633573	$\frac{35-\sqrt{35(15-2\sqrt{30})}}{70}$
	0.527724373779891	$\frac{35-\sqrt{35(15-2\sqrt{30})}}{70}$
	0.029234866294261842	$\frac{35+\sqrt{35(15-2\sqrt{30})}}{70}$
	0.1351279462773748	$\frac{35+\sqrt{35(15-2\sqrt{30})}}{70}$
	0.2599350879809576	$\frac{35+\sqrt{35(15-2\sqrt{30})}}{70}$
	0.08243713410955857	$\frac{35-\sqrt{35(15+2\sqrt{30})}}{70}$
	0.38103682490260515	$\frac{35-\sqrt{35(15+2\sqrt{30})}}{70}$
	0.7329708127268724	$\frac{35-\sqrt{35(15+2\sqrt{30})}}{70}$
	0.006150825401636334	$\frac{35+\sqrt{35(15+2\sqrt{30})}}{70}$
	0.0284300395424344	$\frac{35+\sqrt{35(15+2\sqrt{30})}}{70}$
	0.054688649028481834	$\frac{35+\sqrt{35(15+2\sqrt{30})}}{70}$

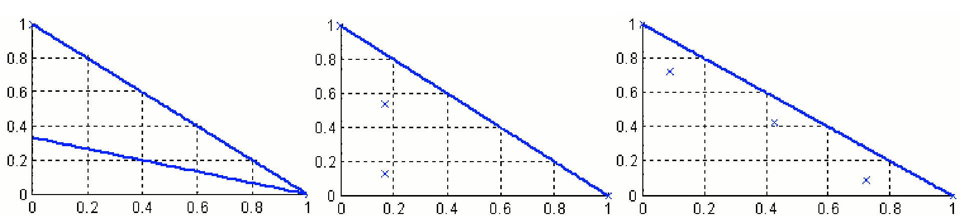

Figure 3.9: Superconvergence points on solid thick lines and points marked by $\times$ on a triangle of type III, $\alpha > 0$ and $\beta = 0$, using $\mathcal{U}_p$, $p = 1$ (left), $p = 2$ (center) and $p = 3$ (right).

Table 3.5: Interior superconvergence points on a triangle of type III, $\alpha > 0$ and $\beta = 0$, using $\mathcal{U}_p$, $p = 2, 3$.

	Xcoordinate	Ycoordinate
$p = 2$	$\frac{1}{6}$ $\frac{1}{6}$	$\frac{4-\sqrt{6}}{12}$ $\frac{4+\sqrt{6}}{12}$
$p = 3$	0.4244522315162876 0.08957869379790769 0.7218160631515568	0.4244522315162876 0.7218160631515568 0.08957869379790769

average at the *outflow* boundary of the domain.

Theorem 3.10. *Under the conditions of Theorem 3.1 the global finite element error e for $p \geq 1$ satisfies the superconvergence result*

$$\int_{\partial\Omega^+} \boldsymbol{a}.\boldsymbol{n} e(x,y) d\sigma = O(h^{2p+1}). \tag{3.178}$$

Proof.

Adding and subtracting $u(x,y)$ to both terms on the left side of (3.7) with $c = 0$ we obtain

$$\int_{\Gamma^-} \boldsymbol{a}.\boldsymbol{n} V(U^- - u + u - U) ds + \iint_\Delta \boldsymbol{a}.\nabla(U - u + u) V dxdy = \iint_\Delta f V dxdy, \quad \forall V \in \mathcal{W}_p, \tag{3.179}$$

where Δ is an arbitrary element. This can be written as

$$\int_{\Gamma^-} \boldsymbol{a}.\boldsymbol{n} V(e - e^-) ds - \iint_\Delta \boldsymbol{a}.\nabla e V dxdy = 0, \quad \forall V \in \mathcal{W}_p, \tag{3.180}$$

Integrating by parts leads to

$$\int_{\Gamma^-} \boldsymbol{a}.\boldsymbol{n} V e^- ds + \int_{\Gamma^+} \boldsymbol{a}.\boldsymbol{n} V e ds - \iint_\Delta \boldsymbol{a}.\nabla V e dxdy = 0, \quad \forall V \in \mathcal{W}_p, \tag{3.181}$$

Testing against $V = 1$ yields

$$\int_{\Gamma^-} \boldsymbol{a}.\boldsymbol{n} e^- ds + \int_{\Gamma^+} \boldsymbol{a}.\boldsymbol{n} e ds = 0. \tag{3.182}$$

Summing over all elements we obtain

$$\int_{\partial\Omega^-} \boldsymbol{a}.\boldsymbol{n} e^- d\sigma + \int_{\partial\Omega^+} \boldsymbol{a}.\boldsymbol{n} e d\sigma = 0. \tag{3.183}$$

Combining (3.183) and Lemma 3.2 we establish (3.178).

Now we investigate the superconvergence properties of the DG solution on meshes consisting of triangles of type III where $[\alpha, \beta]^T$ is parallel to one edge of every element in the mesh.

Without loss of generality we consider the case $[\alpha, \beta]^T = [1, 0]^T$ on uniform triangular meshes obtained by partitioning the domain $\Omega = [0, 1]^2$ into $N = n \times n$ squares and dividing each square into two triangles by connecting the upper-left and lower-right vertices.
Since the characteristics are parallel to the $x-axis$, our problem is equivalent to n decoupled problems on strips parallel to the $x - axis$. For instance, in Figure 3.10 we show the m^{th} strip $[0, 1] \times [(m-1)h, mh]$, $m = 2$, $h = 0.1$, with $2n$ triangles. Let us order the elements in this strip from left to right as Δ_j, $j = 1, 2, ..., 2n$. Similarly, the vertical and oblique edges in the strip are also ordered from left to right as Γ_j, $j = 0, 1, \cdots, 2n$. The horizontal edges are not included here because they are parallel to the characteristics, *i.e.*, $\boldsymbol{a} \cdot \boldsymbol{n} = 0$.

We will show that on the $outflow$ edge, the leading term of the global discretization error on each element is proportional to Legendre polynomial of degree $p + 1$. We further show a strong pointwise superconvergence results on each element. Finally, we show that on average the DG solution exhibits an $O(h^{2p+2})$ strong superconvergence at the $outflow$ boundary of each strip.

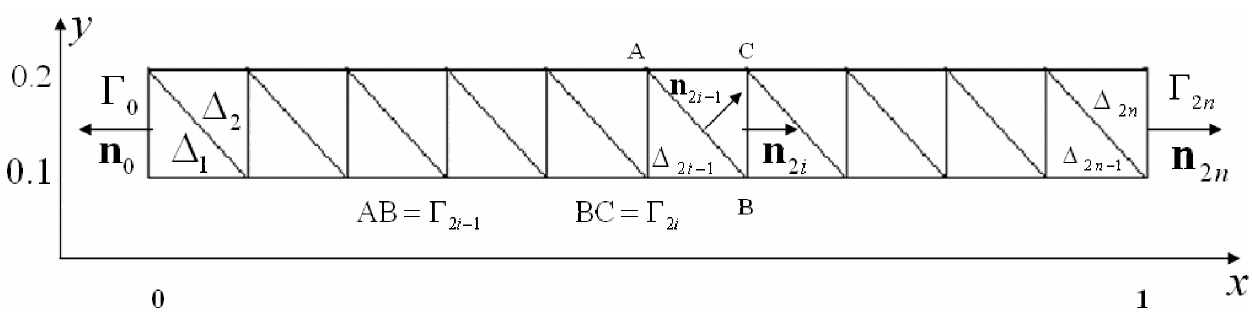

Figure 3.10: A horizontal strip of elements of type III with $[\alpha, \beta] = [1, 0]$.

In the following theorem we state and prove the asymptotic behavior of the global error for the case $\alpha = 1$, $\beta = 0$.

Theorem 3.11. *Let $[\alpha, \beta]^T = [1, 0]^T$ and $c = 0$. Under the conditions of Theorem 3.1 on a uniform mesh as shown in Figure 3.10 with $\mathcal{P}_p$, $p \geq 0$, the leading term of global error on the $outflow$ edge Γ_j of each element (mapped to a canonical element) is such that*

$$Q_{p+1,j}(\xi, \eta) = C_j L_{p+1}(\eta). \tag{3.184}$$

On each element Δ_j we have

$$e = u - U = \sum_{k=p+1}^{\infty} Q_{p+1,j}(\xi, \eta) h^k, \tag{3.185}$$

where

$$Q_{p+1,j}(\xi,\eta) = \sum_{i=0}^{p} c_{i,j}^{p} \varphi_{p-i,j}^{i}(\xi,\eta) + \sum_{i=0}^{p+1} c_{i,j}^{p+1} \varphi_{p+1-i,j}^{i}(\xi,\eta). \tag{3.186}$$

Furthermore, if $U^-|_{\Gamma^-} = \pi u$ as in Lemma 3.2, then (3.37) still holds on each strip as

$$\int_{\Gamma_{2n}} \boldsymbol{a}.\boldsymbol{n}_{2n} e ds = O(h^{2p+2}). \tag{3.187}$$

Proof. We consider the strip in Figure 3.10 with $2n$ elements and construct the space $\mathcal{S}^{2n,p}$ consisting of piecewise polynomial functions

$$\mathcal{S}^{2n,p} = \{V \mid V|_{\Delta_j} = V_j \in \mathcal{P}_p,\ j = 1,\cdots,2n\}. \tag{3.188}$$

The orthogonality condition (3.13) on an element Δ_j in the strip becomes on

$$\int_{\Gamma_j} \boldsymbol{a}.\boldsymbol{n}_j e V_j ds + \int_{\Gamma_{j-1}} \boldsymbol{a}.\boldsymbol{n}_{j-1} e^- V_j ds - \iint_{\Delta_j} \boldsymbol{a}.\nabla V_j e dxdy = 0, \quad \forall\ V_j \in \mathcal{P}_p, \tag{3.189}$$

where we have used the fact that $\int_\Gamma \boldsymbol{a}.\boldsymbol{n} e^- V_j ds = 0$ on each horizontal edge.
Summing over the elements, $j = 1,\cdots,2n$, we obtain the edge orthogonality

$$-\sum_{j=1}^{2n} \int_{\Gamma_j} \boldsymbol{a}.\boldsymbol{n}_j e^-[V] ds + \int_{\Gamma_{2n}} \boldsymbol{a}.\boldsymbol{n}_{2n} e V ds$$

$$-\int_{\Gamma_0} \boldsymbol{a}.\boldsymbol{n}_0 e^- V ds - \sum_{j=1}^{2n} \iint_{\Delta_j} \boldsymbol{a}.\nabla V e dxdy = 0, \quad \forall\ V \in \mathcal{S}^{2n,p}, \tag{3.190}$$

where the normal vectors are such $\boldsymbol{n}_j > 0$, $e^-|_{\Gamma_j}$ is the limit from the element Δ_j and

$$[V]|_{\Gamma_j} = V_{j+1}|_{\Gamma_j} - V_j|_{\Gamma_j},$$

is the jump of V across the edge Γ_j.

Now let $q(x)$ be an arbitrary polynomial of degree p and consider the adjoint problem on the strip consisting of union $S = \cup_{j=1}^{2n} \Delta_j$

$$-\boldsymbol{a} \cdot \nabla V^* = 0, \qquad (x,y) \in S$$

subject to the boundary conditions $V^*|_{\Gamma_{2n}} = q(y)$ where Γ_{2n} is the vertical edge $x = x_n = 1$. We note that the analysis for other vertical and oblique edges follows the same line of reasoning.

Since exact solution $V^*(x,y) = q(y) \in \mathcal{P}_p$ is continuous, we set $V = V^*$ in (3.190)

$$\int_{\Gamma_{2n}} \boldsymbol{a}.\boldsymbol{n}_{2n} e q ds - \int_{\Gamma_0} \boldsymbol{a}.\boldsymbol{n}_0 e^- q ds = 0, \qquad \forall\ q \in \mathbf{P}_p. \tag{3.191}$$

If $e^{-}|_{\Gamma_0} = 0$, the error e is orthogonal to all $q \in \mathbf{P}_p$ on Γ_{2n}, *i.e.*,

$$\int_{\Gamma_{2n}} \boldsymbol{a}.\boldsymbol{n}_{2n} eqds = 0, \qquad \forall\ q \in \mathbf{P}_p. \tag{3.192}$$

Following the same line of reasoning one can prove a similar result for each vertical or oblique edge in the strip.

Furthermore, the edge orthogonality condition (3.192) leads to the element orthogonality condition Δ_j

$$\iint_{\Delta_j} \boldsymbol{a}.\nabla V edxdy = 0, \quad \forall\ V \in \mathcal{P}_p. \tag{3.193}$$

Now we replace the global error, $e = u - U$, in (3.192) and (3.193) by its Maclaurin series (3.15) and collect terms having same powers of h.
From this point on, the proof is the same as for the local error in Theorems 3.1 and 3.2. Thus, we establish (3.184), (3.185) and (3.186).
Finally, let $U^{-}|_{\Gamma^{-}} = \pi u$ as in Lemma 3.2 and combine (3.191) with Lemma 3.2 to establish (3.187). □

Corollary 3.5. *Under the assumptions of Theorem 3.11 the DG solution on an arbitrary element Δ_j in the strip of elements of type III is $O(h^{p+2})$ superconvergent at the points given in Corollary 3.2 shifted to Δ_j.*

Proof. Proof is the same as for Corollary 3.2 □

Remark: If $U \in \mathcal{U}_p$ on meshes consisting of elements of type III, the DG solution is $O(h^{p+2})$ at every point of the $outflow$ edges of the mesh.

In the next examples we will show several computational results to validate the previous theorem. We will present a superconvergence analysis of the local error. These superconvergence results still hold on meshes consisting of elements of type III only. In order to maintain these superconvergence rates for the global solution on general meshes one needs to use $O(h^{p+2})$ approximations of the boundary conditions at the $inflow$ boundary of every element. This is possible on elements whose $inflow$ edges are on the $inflow$ boundary of the domain while on the remaining elements we correct the solution by adding an error estimate and use it as an $inflow$ boundary condition. This will be discussed in Chapter 4.

3.7 Computational Examples

In the following examples we use the exact boundary conditions at the $inflow$ boundary. The use of polynomials interpolating the exact boundary conditions at the roots of $(p+1)$-degree Legendre polynomials yields similar results. Thus, here we present results for the exact boundary conditions only. We will consider meshes consisting of elements of type III only where each triangle has one side parallel to the characteristics. On the space $\mathcal{P}_p$ we compute the maximum error at the shifted roots of the $(p+1)$-degree Legendre polynomial over all $outflow$ edges. If U is in $\mathcal{V}_p$, we compute the maximum error at the shifted Legendre roots and interior points given by (3.105). If U is in $\mathcal{U}_p$, the maximum error is computed at 15 uniformly distributed points on each $outflow$ edge and the interior superconvergence points shown in Figure 3.9 and Table 3.5. For all spaces the maximum error at the superconvergence points is denoted by $||e||_\infty^*$. Meshes consisting of elements of all types will be considered later on.

Example 3.1.

Let us consider the linear problem with characteristics parallel to the $x-axis$.

$$u_x + u = f(x,y), \qquad (x,y) \in \Omega = [0,1]^2, \tag{3.194a}$$

subject to the boundary conditions

$$u(0,y) = g(y). \tag{3.194b}$$

We select $f(x,y)$ and g such that the exact solution is

$$u(x,y) \;=\; e^{3x\,+\,2y\,-\,1}. \tag{3.194c}$$

We solve this problem on uniform triangular meshes having $N = 32, 72, 128$ elements obtained by partitioning the domain Ω into $n \times n$, $n = 4, 6, 8$, squares and divide each square into two triangles by connecting the upper left and lower right vertices. Thus, each element of this mesh is of type III, *i.e.,* it has one side parallel to the characteristic. We compute the finite element solutions with the exact boundary condition $U^- = u$ in the spaces $\mathcal{P}_p$, $\mathcal{V}_p$ and $\mathcal{U}_p$ with $p = 0$ to 3 and plot the zero-level curves of the true error on each element in Figures 3.11- 3.16. We observe that the zero-level curves pass through the superconvergence points marked by $\times$. The maximum errors at the superconvergence points as well as their order of convergence are shown in Table 3.6. These results indicate that the DG solution is $O(h^{p+2})$ superconvergent at the superconvergence points while globally it is only $O(h^{p+1})$ convergent. This is in full agreement with the theory. We note that $\mathcal{P}_1 = \mathcal{U}_0$ and $\mathcal{P}_0 = \mathcal{V}_0$ yield the same errors.

Example 3.2.

We consider the following linear hyperbolic problem

$$u_x + u_y = f(x,y), \qquad (x,y) \in \Omega = [0,1]^2, \tag{3.195a}$$

subject to the boundary conditions

$$u(x,0) = g_0(x), \quad u(0,y) = g_1(y). \tag{3.195b}$$

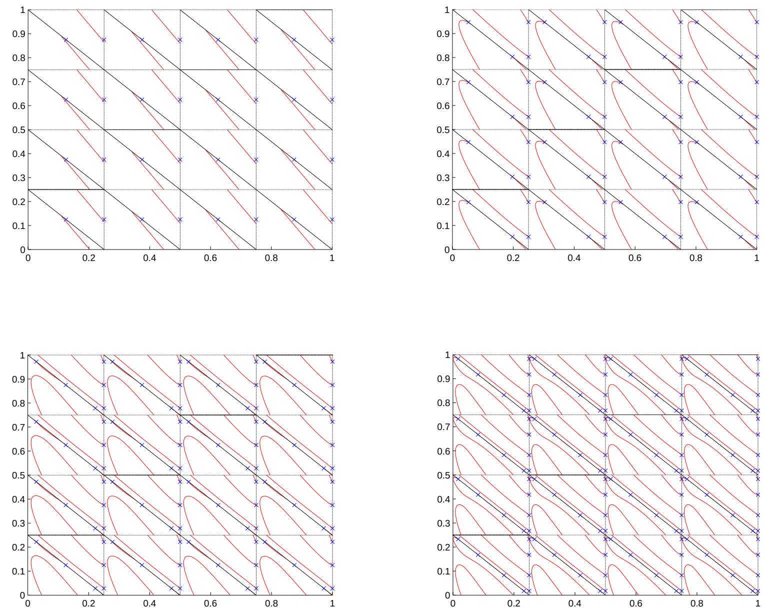

Figure 3.11: Zero-level curves of the true error for Example 3.1 on a mesh having $N = 32$ elements using the spaces $\mathcal{P}_p,\ p = 0, 1, 2, 3$ (upper left to lower right).

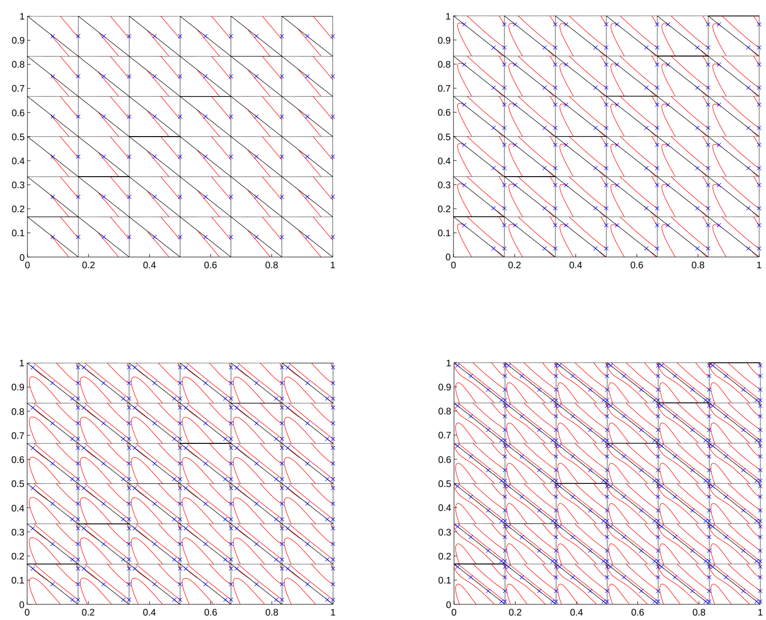

Figure 3.12: Zero-level curves of the true error for Example 3.1 on a mesh having $N = 72$ elements using the spaces $\mathcal{P}_p,\ p = 0, 1, 2, 3$ (upper left to lower right).

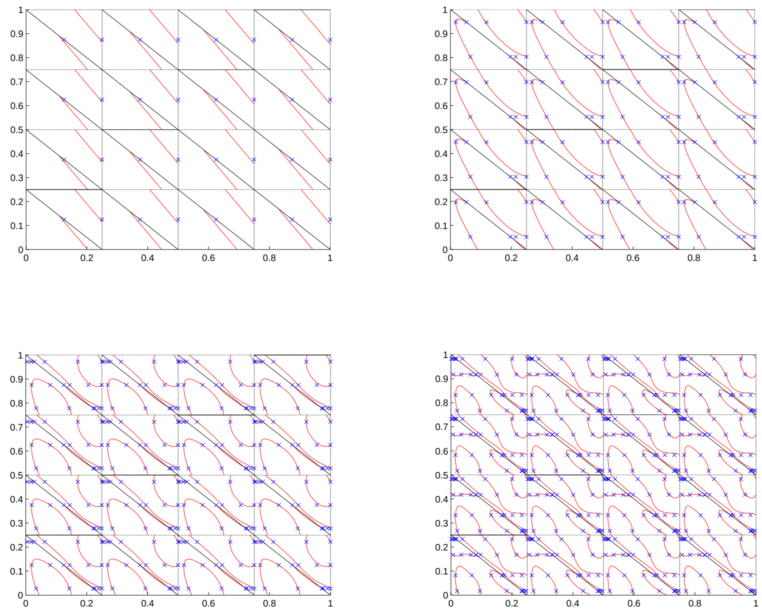

Figure 3.13: Zero-level curves of the true error for Example 3.1 on a mesh having $N = 32$ elements using the spaces $\mathcal{V}_p,\ p = 0, 1, 2, 3$ (upper left to lower right).

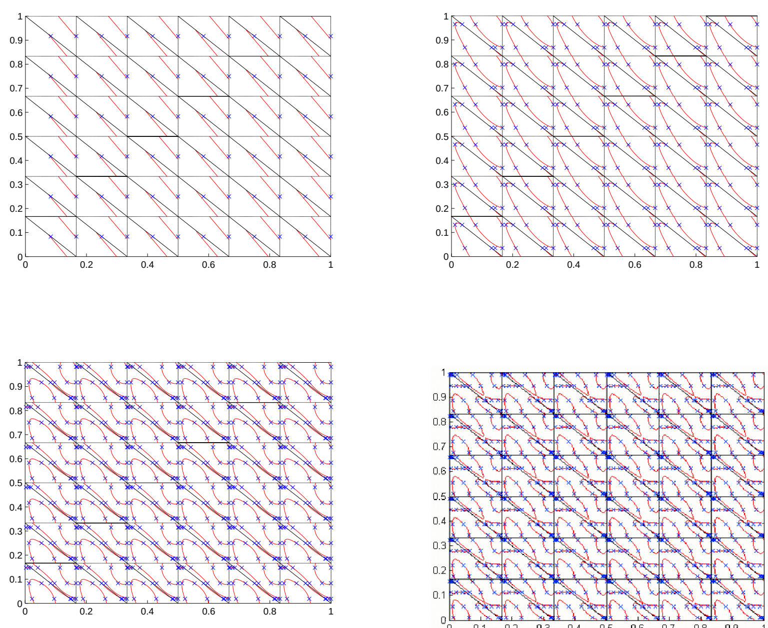

Figure 3.14: Zero-level curves of the true error for Example 3.1 on a mesh having $N = 72$ elements using the spaces $\mathcal{V}_p,\ p = 0, 1, 2, 3$ (upper left to lower right).

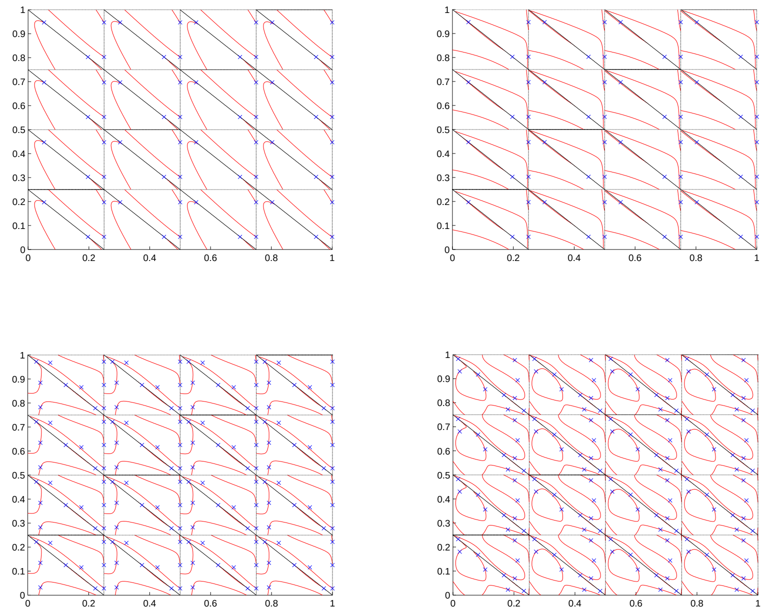

Figure 3.15: Zero-level curves of the true error for Example 3.1 on a mesh having $N = 32$ elements using the spaces $\mathcal{U}_p$, $p = 0, 1, 2, 3$ (upper left to lower right).

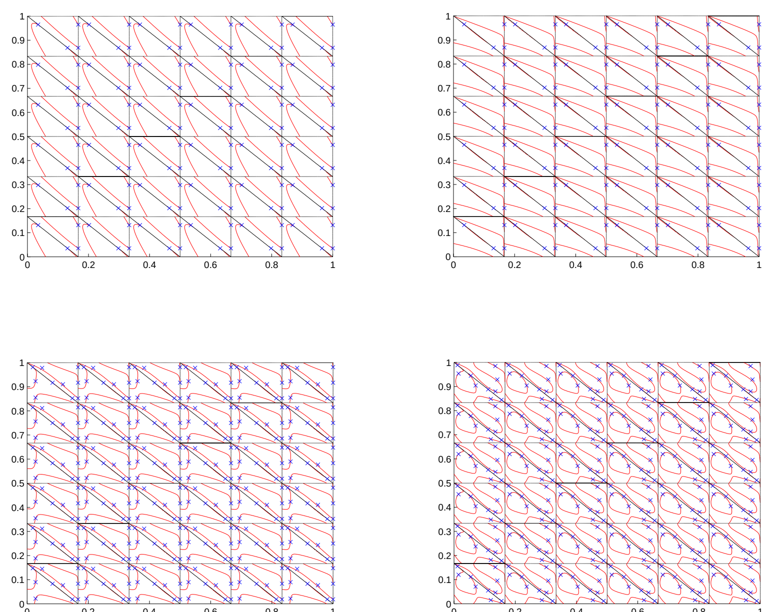

Figure 3.16: Zero-level curves of the true error for Example 3.1 on a mesh having $N = 72$ elements using the spaces $\mathcal{U}_p$, $p = 0, 1, 2, 3$ (upper left to lower right).

Table 3.6: Maximum errors and orders of convergence at the superconvergence points for Example 3.1 on uniform meshes having $N = 32, 72, 128$ elements.

$\mathcal{P}_p$				
N	$p=0$	$p=1$	$p=2$	$p=3$
32	4.3680e-3	2.9896e-4	4.5803e-6	9.2263e-8
72	2.0612e-3	9.2804e-5	9.4682e-7	1.2544e-8
128	1.1940e-3	4.0109e-5	3.0532e-7	3.0070e-9
rate	1.8699	2.8971	3.9058	4.9381
$\mathcal{V}_p$				
N	$p=0$	$p=1$	$p=2$	$p=3$
32	4.3680e-3	1.0864e-4	1.9520e-6	8.0246e-8
72	2.0612e-3	3.3138e-5	3.9776e-7	1.1600e-8
128	1.1940e-3	1.4173e-5	1.2766e-7	2.9560e-9
rate	1.8699	2.9376	3.7832	4.7631
$\mathcal{U}_p$				
N	$p=1$	$p=2$	$p=3$	$p=4$
32	4.2903e-2	1.5433e-3	4.3129e-5	7.5285e-7
72	1.3952e-2	3.3389e-4	6.2795e-6	3.0969e-7
128	6.1686e-3	1.1061e-4	1.6244e-6	1.0472e-8
rate	2.8082	3.8045	4.7339	5.9197

We select $f(x, y)$, g_0 and g_1 such that the exact solution is $u(x, y) = sin(2x - 3y)$. We solve this problem on uniform triangular meshes having $N = 32, 72, 128, 200$ elements obtained by subdividing Ω into $n \times n$, $n = 4, 6, 8, 10$, squares and using diagonals parallel to $y = x$ to split each square into two triangles. We compute finite element solutions in the spaces $\mathcal{P}_p$, $\mathcal{V}_p$ and $\mathcal{U}_p$ with $p = 0$ to 3 and plot the zero-level curves of the error in Figures 3.17, 3.18 and 3.19. Superconvergence points marked by $\times$ are points where the leading term of the true DG error is zero. Thus, in general, the true DG error is not zero at the superconvergence points. Our results show that on most elements the zero-level curves of the true error pass close to the superconvergence points. Under mesh refinement the zero-level curves get closer to these points. The maximum errors at the superconvergence points as well as their order of convergence shown in Table 3.7 indicate that the DG solution is $O(h^{p+2})$ superconvergent at the superconvergence points while globally it is only $O(h^{p+1})$ convergent as shown in Table 3.8. This is in full agreement with the theory. We note that $\mathcal{P}_1 = \mathcal{U}_0$ and $\mathcal{V}_0 = \mathcal{P}_0$ yield the same errors.

Example 3.3.

We consider the following linear hyperbolic problem

$$3u_x + u_y = f(x, y), \qquad (x, y) \in \Omega = [0, 1]^2, \tag{3.196a}$$

subject to the boundary conditions

$$u(x, 0) = g_0(x), \quad u(0, y) = g_1(y). \tag{3.196b}$$

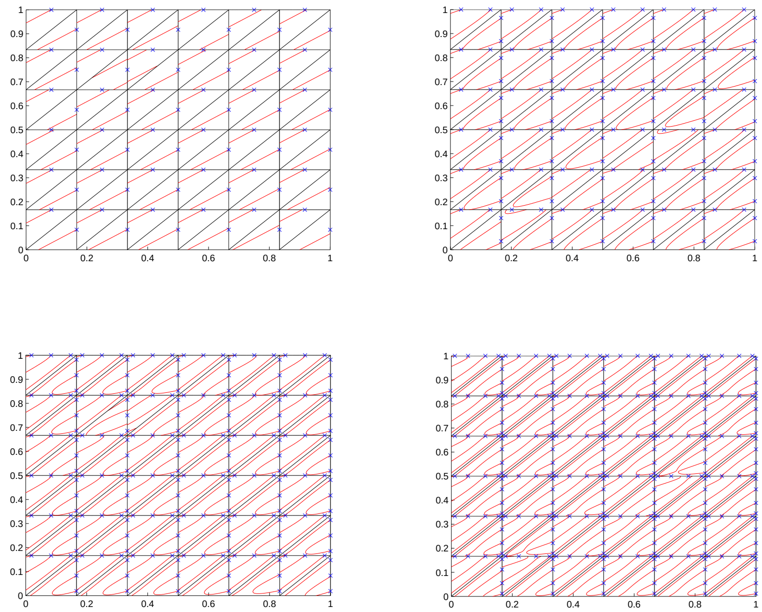

Figure 3.17: Zero-level curves of the true error for Example 3.2 on uniform meshes having $N = 72$ elements using $\mathcal{P}_p,\ p = 0$ to 3 (upper left to lower right).

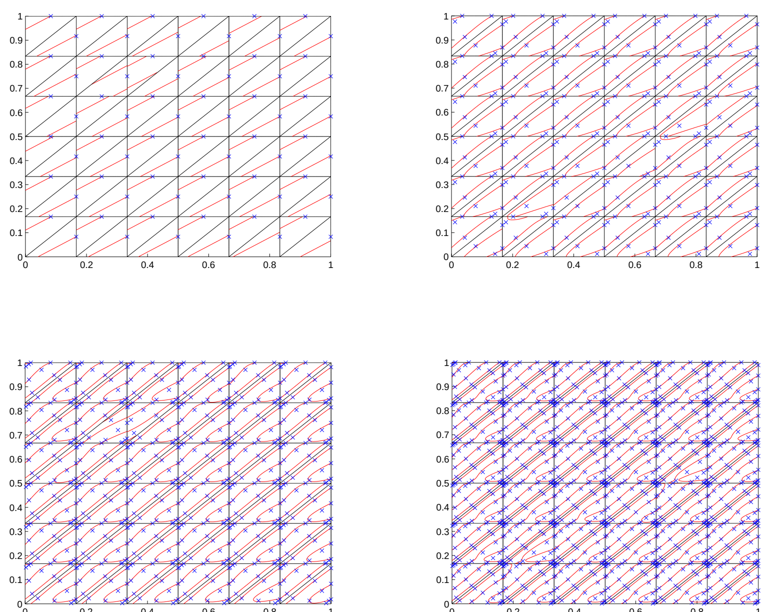

Figure 3.18: Zero-level curves of the true error for Example 3.2 on uniform meshes having $N = 72$ elements using $\mathcal{V}_p,\ p = 0$ to 3 (upper left to lower right).

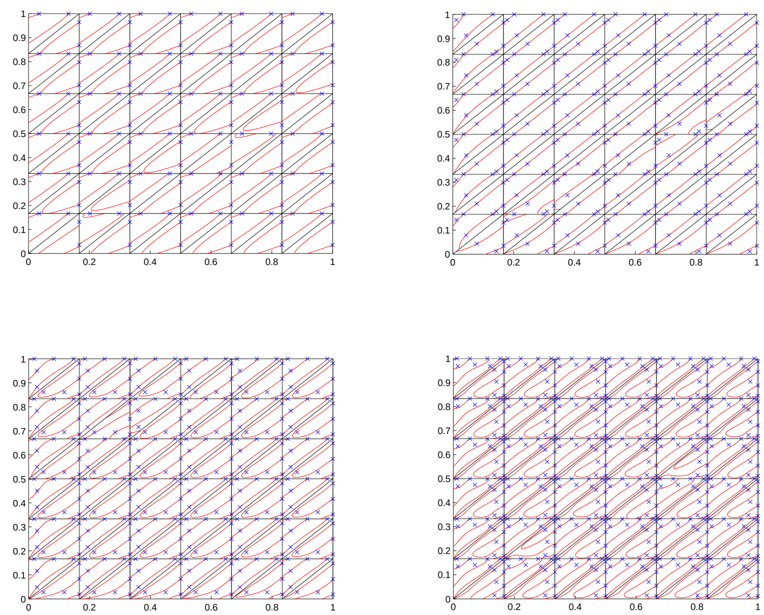

Figure 3.19: Zero-level curves of the true error for Example 3.2 on uniform meshes having $N = 72$ elements using $\mathcal{U}_p$, $p = 0$ to 3 (upper left to lower right).

Table 3.7: Maximum errors and orders of convergence at the superconvergence points for Example 3.2 on uniform meshes having $N = 32, 72, 128, 200$ elements.

	$\mathcal{P}_p$							
N	$p=0$		$p=1$		$p=2$		$p=3$	
	$\|\|e\|\|_\infty^*$	order	$\|\|e\|\|_\infty^*$	order	$\|\|e\|\|_\infty^*$	order	$\|\|e\|\|_\infty^*$	order
32	2.3239e-2		1.3404e-3		1.1058e-5		2.3056e-6	
72	1.0383e-2	1.9869	3.9926e-4	2.9871	2.1960e-6	3.9870	3.1827e-7	4.8838
128	5.8488e-3	1.9951	1.6874e-4	2.9936	6.9659e-7	3.9912	7.7805e-8	4.8967
200	3.7449e-3	1.9980	8.6472e-5	2.9962	2.8556e-7	3.9963	2.5843e-8	4.9392
	$\mathcal{V}_p$							
32	2.3239e-2		3.8042e-4		1.3878e-5		1.7157e-6	
72	1.0383e-2	1.9869	1.1295e-4	2.9949	2.7460e-6	3.9959	2.3086e-7	4.9470
128	5.8488e-3	1.9951	4.7686e-5	2.9974	8.7009e-7	3.9951	5.6951e-8	4.9267
200	3.7449e-3	1.9980	2.4424e-5	2.9984	3.5686e-7	3.9941	1.8994e-8	4.9209
	$\mathcal{U}_p$							
32	1.3404e-3		3.9944e-4		1.1119e-5		5.1173e-7	
72	3.9926e-4	2.9871	1.1860e-4	2.9949	2.1996e-6	3.9964	6.9265e-8	4.9322
128	1.6874e-4	2.9936	5.0070e-5	2.9975	6.9609e-7	3.9994	1.6618e-8	4.9619
200	8.6472e-5	2.9962	2.5644e-5	2.9985	2.8555e-7	3.9931	5.5092e-9	4.9478

Table 3.8: $\|u - U\|_{\mathcal{L}^2}$ and the order of convergence over the whole domain for Example 3.2 on uniform meshes having $N = 32, 72, 128, 200$ elements.

	$\mathcal{P}_p$							
N	$p=0$		$p=1$		$p=2$		$p=3$	
	$\|\|e\|\|_2$	order	$\|\|e\|\|_2$	order	$\|\|e\|\|_2$	order	$\|\|e\|\|_2$	order
32	3.0712e-1		8.0179e-2		1.7625e-2		3.0925e-3	
72	2.0736e-1	0.9687	3.6039e-2	1.9722	5.2674e-3	2.9787	6.1501e-4	3.9834
128	1.5622e-1	0.9845	2.0351e-2	1.9864	2.2289e-3	2.9894	1.9504e-4	3.9919
200	1.2523e-1	0.9907	1.3048e-2	1.9919	1.1428e-3	2.9936	7.9975e-5	3.9953
	$\mathcal{V}_p$							
32	3.0712e-1		8.4682e-2		2.0598e-2		4.1127e-3	
72	2.0736e-1	0.9687	3.8044e-2	1.9734	6.1537e-3	2.9797	8.1614e-4	3.9886
128	1.5622e-1	0.9845	2.1480e-2	1.9870	2.6037e-3	2.9898	2.5861e-4	3.9949
200	1.2523e-1	0.9907	1.3770e-2	1.9923	1.3349e-3	2.9938	1.0602e-4	3.9960
	$\mathcal{U}_p$							
32	8.0179e-2		7.1266e-2		1.7284e-2		3.0816e-3	
72	3.6039e-2	1.9722	3.2258e-2	1.9549	5.1734e-3	2.9751	6.1304e-4	3.9826
128	2.0351e-2	1.9864	1.8278e-2	1.9747	2.1908e-3	2.9868	1.9445e-4	3.9914
200	1.3048e-2	1.9919	1.1742e-2	1.9831	1.1238e-3	2.9916	7.9739e-5	3.9949

We select $f(x, y),\ g_0$ and g_1 such that the exact solution is

$$u(x, y) \ = e^{x+2y}. \tag{3.196c}$$

We solve this problem on triangular meshes having $N = 96, 216, 384, 600$ elements obtained by dividing Ω into $n \times 3n,\ n = 4, 6, 8, 10$ rectangles and using diagonals parallel to $y = x/3$ to split each rectangle into two triangles. Thus, each element of this mesh is of type III. We use $\mathcal{P}_p,\ \mathcal{V}_p$ and $\mathcal{U}_p$ with $p = 0$ to 3 and present the maximum errors at the superconvergence points as well as their order of convergence in Table 3.9 to observe $O(h^{p+2})$ convergence rates. In Figure 3.20 we plot the zero-level curves of the true error on each element. The superconvergence points are marked by $\times$. These results indicate that the DG solution is $O(h^{p+2})$ globally superconvergent at the superconvergence points which is in full agreement with Theorem 3.11. We note that the error in the $\mathcal{L}^2$ norm is only $O(h^{p+1})$.

Example 3.4.

We consider the following problem with a contact discontinuity

$$2u_x + u_y = 0, \qquad (x, y) \in \Omega = [0, 1]^2, \tag{3.197a}$$

subject to the boundary conditions

$$u(x, 0) = e^{-x}, \qquad 0 \le x \le 1, \tag{3.197b}$$

$$u(0, y) = e^{2y} + .25, \qquad 0 < y \le 1. \tag{3.197c}$$

Table 3.9: Maximum error and order of convergence at superconvergence points for Example 3.3 on meshes having $N = 96, 216, 384, 600$ elements.

$\mathcal{P}_p$								
N	$p=0$		$p=1$		$p=2$		$p=3$	
	$\|\|e\|\|_\infty^*$	order	$\|\|e\|\|_\infty^*$	order	$\|\|e\|\|_\infty^*$	order	$\|\|e\|\|_\infty^*$	order
96	4.6196e-2		8.7313e-4		1.2136e-5		1.9424e-7	
216	2.1395e-2	1.8983	2.7122e-4	2.8835	2.5144e-6	3.8824	2.6369e-7	4.9250
384	1.2286e-2	1.9281	1.1716e-4	2.9177	8.1484e-7	3.9169	6.3532e-9	4.9473
600	7.9618e-3	1.9443	6.0849e-5	2.9362	3.3858e-7	3.9356	2.1011e-9	4.9586
$\mathcal{V}_p$								
96	4.6196e-2		9.0521e-4		1.2616e-5		8.4459e-8	
216	2.1395e-2	1.8983	2.7782e-4	2.9131	2.5802e-6	3.9143	1.1440e-8	4.9303
384	1.2286e-2	1.9281	1.1929e-4	2.9386	8.3077e-7	3.9393	2.7530e-9	4.9516
600	7.9618e-3	1.9443	6.1733e-5	2.9524	3.4387e-7	3.9530	9.0859e-10	4.9680
$\mathcal{U}_p$								
96	8.7313e-4		2.7782e-4		1.5465e-5		2.5853e-7	
216	2.7122e-4	2.8835	8.4283e-5	2.9418	3.1837e-6	3.8982	3.5274e-8	4.9125
384	1.1716e-4	2.9177	3.5979e-5	2.9589	1.0284e-6	3.9280	8.5200e-9	4.9386
600	6.0849e-5	2.9362	1.8553e-5	2.9682	4.2651e-7	3.9443	2.8222e-9	4.9515

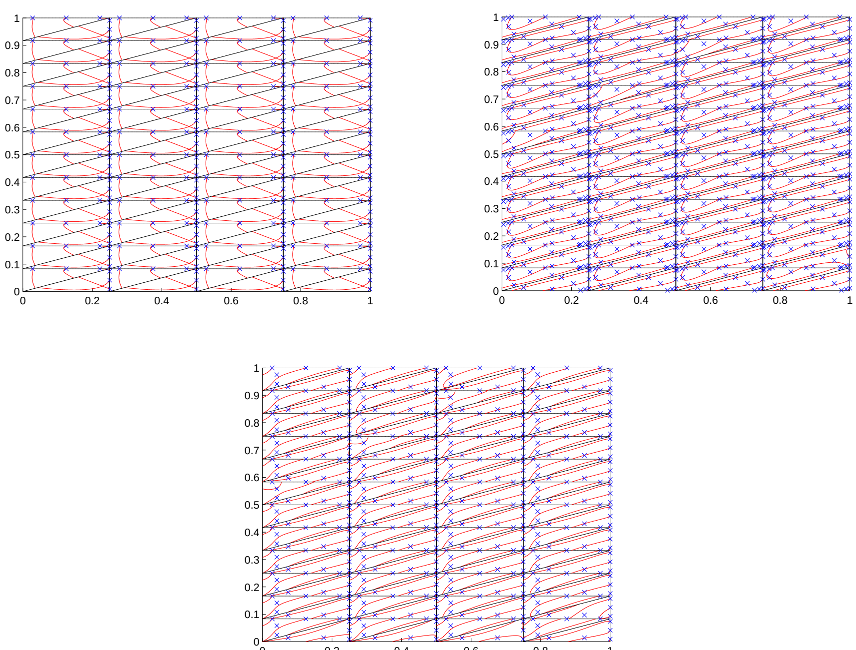

Figure 3.20: Zero-level curves of the true error for Example 3.3 on uniform meshes having $N = 96$ elements using $\mathcal{P}_2$ (top left), $\mathcal{V}_2$ (top right) and $\mathcal{U}_2$ (bottom).

The exact solution is

$$u(x,y) = \begin{cases} e^{-x+2y} + .25 & \text{if } x < 2y, \\ e^{-x+2y} & \text{if } x \geq 2y. \end{cases} \tag{3.197d}$$

The true solution has a contact discontinuity along $y = x/2$. We solve this problem on triangular meshes having $N = 64, 144, 256, 400$ elements obtained by dividing Ω into $n \times 2n,\ n = 4, 6, 8, 10$, rectangles and using diagonals parallel to $y = x/2$ to split each rectangle into two triangles. We note that our meshes are aligned with the discontinuity. Therefore, as a result we expect the superconvergence properties are still valid. We compute finite element solutions in $\mathcal{P}_p, \mathcal{V}_p$, and $\mathcal{U}_p$, $p = 0$ to 3. We observe that the zero-level curves plotted in Figure 3.21 pass close the superconvergence points marked by $\times$. The maximum errors at the superconvergence points and their order of convergence shown in Table 3.10 indicate that the DG solution is $O(h^{p+2})$ superconvergent at the shifted roots of Legendre polynomials on the *outflow* edges and at the interior superconvergence points for $\mathcal{V}_p$ and $\mathcal{U}_p$. These results are in full agreement with the theory where the mesh is aligned with the discontinuity. We note that the error in the $\mathcal{L}^2$ norm is $O(h^{p+1})$.

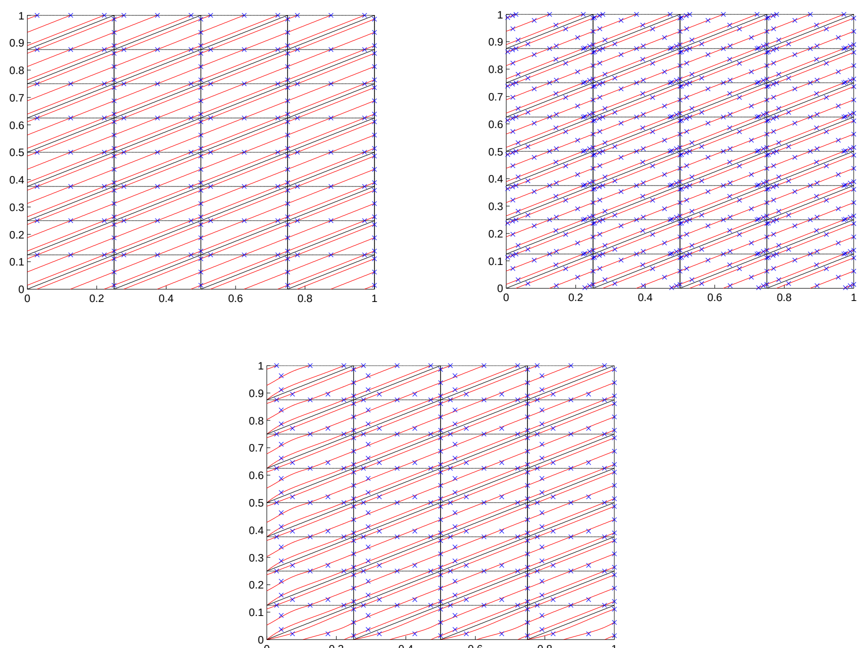

Figure 3.21: Zero-level curves of the true error for Example 3.4 on uniform meshes having $N = 64$ elements using $\mathcal{P}_2$(top left), $\mathcal{V}_2$ (top right) and $\mathcal{U}_2$ (bottom).

Example 3.5.

Table 3.10: Maximum error and order of convergence at the superconvergence points for Example 3.4 on uniform meshes having $N = 64, 144, 256, 400$ elements.

	$\mathcal{P}_p$							
N	$p=0$		$p=1$		$p=2$		$p=3$	
	$\|\|e\|\|_\infty^*$	order	$\|\|e\|\|_\infty^*$	order	$\|\|e\|\|_\infty^*$	order	$\|\|e\|\|_\infty^*$	order
64	1.6994e-2		3.2121e-4		4.4644e-6		5.0457e-8	
144	7.8710e-3	1.8983	9.9778e-5	2.8835	9.2498e-7	3.8823	6.9664e-9	4.8833
256	4.5200e-3	1.9281	4.3103e-5	2.9177	2.9975e-7	3.9168	1.6928e-9	4.9177
400	2.9289e-3	1.9443	2.2385e-5	2.9362	1.2455e-7	3.9357	5.6558e-10	4.9129
	$\mathcal{V}_p$							
64	1.6994e-2		3.3300e-4		4.6407e-6		6.9891e-8	
144	7.8710e-3	1.8983	1.0220e-4	2.9131	9.4917e-7	3.9141	9.5700e-9	4.9038
256	4.5200e-3	1.9281	4.3887e-5	2.9386	3.0561e-7	3.9393	2.3158e-9	4.9320
400	2.9289e-3	1.9443	2.2710e-5	2.9524	1.2649e-7	3.9531	7.6959e-10	4.9370
	$\mathcal{U}_p$							
64	3.2121e-4		3.3300e-4		5.6889e-6		6.8908e-8	
144	9.9778e-5	2.8835	1.0220e-4	2.9131	1.1711e-6	3.8980	9.4800e-9	4.8921
256	4.3103e-5	2.9177	4.3887e-5	2.9386	3.7832e-7	3.9280	2.2994e-9	4.9238
400	2.2385e-5	2.9362	2.2710e-5	2.9524	1.5689e-7	3.9445	7.7014e-10	4.9021

We consider the following problem with a contact discontinuity

$$2u_x + u_y = 0, \qquad (x, y) \in [0, 1]^2, \tag{3.198a}$$

subject to the boundary conditions

$$u(x, 0) = e^{-x}, \qquad 0 \le x \le 1, \tag{3.198b}$$

$$u(0, y) = \begin{cases} e^{2y} & \text{if } 0 < y \le 0.035, \\ e^{2y} + 0.035 & \text{if } 0.035 < y \le 1. \end{cases} \tag{3.198c}$$

The exact solution is

$$u(x, y) = \begin{cases} e^{-x+2y} + 0.035 & \text{if } x/2 + 0.035 < y, \\ e^{-x+2y} & \text{if } x/2 + 0.035 \ge y. \end{cases} \tag{3.198d}$$

The true solution has a contact discontinuity along $y = x + 0.035$.

We solve this problem using the same parameters and meshes as for Example 3.4. In this example our meshes are parallel but not aligned with the discontinuity which intersects one strip of elements only and does not affect the behavior of the error in elements outside the strip. In Figure 3.22 we plot the zero-level curves of the true error on each element for $N = 64$ and $p = 0$, to 3. We present the maximum errors at the superconvergence points over all elements and their order of convergence in Table 3.11 which exhibit low convergence rates. However, the maximum errors at superconvergence points over elements not containing the discontinuity presented in Table 3.12 indicate that DG solutions are $O(h^{p+2})$ superconvergent at the points marked by $\times$ away from the discontinuity as well as on the $outflow$ edges for $U \in \mathcal{U}_p$.

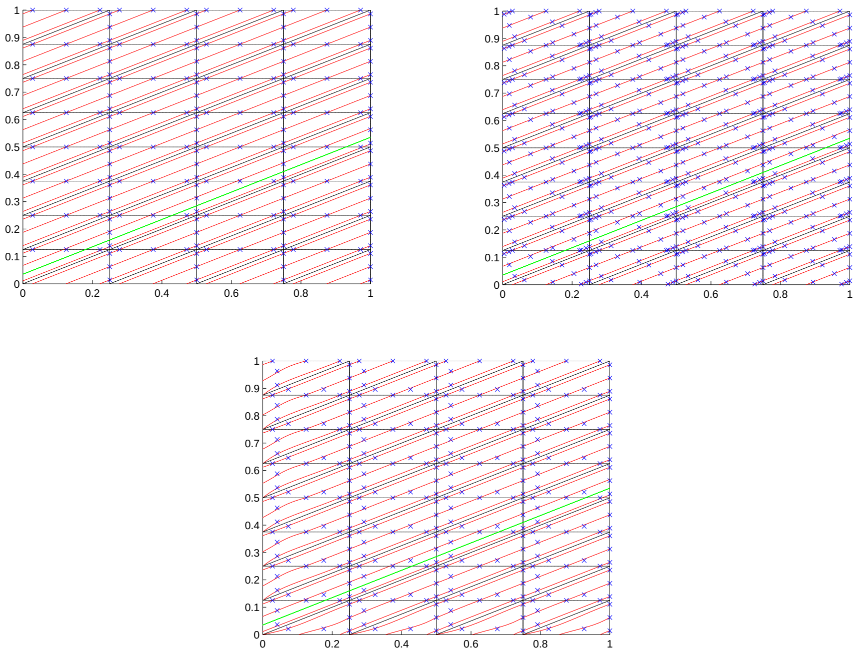

Figure 3.22: Zero-level curves of the true error for Example 3.5 on uniform meshes having $N = 64$ elements using $\mathcal{P}_2$(top left), $\mathcal{V}_2$ (top right) and $\mathcal{U}_2$ (bottom).

Table 3.11: Maximum error and order of convergence at the superconvergence points on all elements for Example 3.5 on uniform meshes having $N = 64, 144, 256, 400$ elements.

$\mathcal{P}_p$								
N	$p=0$		$p=1$		$p=2$		$p=3$	
	$\|\|e\|\|_\infty^*$	order	$\|\|e\|\|_\infty^*$	order	$\|\|e\|\|_\infty^*$	order	$\|\|e\|\|_\infty^*$	order
64	1.6994e-2		2.5825e-3		3.2917e-3		2.4563e-3	
144	1.2878e-2	0.6840	4.8655e-4	4.1167	1.9806e-3	1.2528	2.0893e-3	0.3991
256	1.1503e-2	0.8622	4.1568e-3	-7.4567	2.6711e-3	-1.0395	5.7284e-3	-3.5059
400	1.1337e-2	1.6828	2.1135e-3	3.0311	8.7969e-4	4.9774	2.9636e-3	2.9534
$\mathcal{V}_p$								
64	1.6994e-2		1.8091e-2		1.3921e-3		2.1798e-3	
144	1.2878e-2	0.6840	3.3750e-3	4.1410	1.5815e-2	-5.9934	2.2122e-3	-0.0364
256	1.6503e-2	0.8622	2.9732e-2	-7.5634	2.6475e-3	6.2128	3.9529e-4	5.9863
400	1.1337e-2	1.6828	2.1135e-3	11.8483	9.7209e-4	4.4901	1.3434e-3	-5.4823
$\mathcal{U}_p$								
64	2.5825e-3		1.9500e-2		2.3507e-2		3.4658e-3	
144	4.8655e-4	4.1167	4.0967e-3	3.8480	1.5815e-2	0.9776	4.6916e-3	-0.7468
256	4.1568e-3	-7.4567	3.0140e-2	-6.9371	1.8910e-2	-0.6214	1.5148e-2	-4.0743
400	2.1135e-3	3.0311	1.1088e-2	4.4814	3.8052e-3	7.1854	8.5259e-3	2.5758

Table 3.12: Maximum error and order of convergence at the superconvergence points on elements not containing the solution discontinuity for Example 3.5 on uniform meshes having $N = 64, 144, 256, 400$ elements.

$\mathcal{P}_p$								
N	$p=0$		$p=1$		$p=2$		$p=3$	
	$\|\|e\|\|_\infty^*$	order	$\|\|e\|\|_\infty^*$	order	$\|\|e\|\|_\infty^*$	order	$\|\|e\|\|_\infty^*$	order
64	1.6994e-2		3.2120e-4		4.4644e-6		6.8842e-8	
144	7.8710e-3	1.8983	9.9778e-5	2.8835	9.2498e-7	3.8823	9.5998e-9	4.8588
256	4.5200e-3	1.9281	4.3103e-5	2.9177	2.9977e-7	3.9166	2.2839e-9	4.9911
400	2.9289e-3	1.9443	2.2385e-5	2.9362	1.2457e-7	3.9354	7.5590e-10	4.9554
$\mathcal{V}_p$								
64	1.6994e-2		1.2250e-4		1.6423e-6		5.0408e-8	
144	7.8710e-3	1.8983	3.7599e-5	2.9131	3.4028e-7	3.8822	7.0560e-9	4.8494
256	4.5200e-3	1.9281	1.6145e-5	2.9386	1.1028e-7	3.9167	1.6814e-9	4.9854
400	2.9289e-3	1.9443	8.3547e-6	2.9524	4.5806e-8	3.9373	5.6110e-10	4.9185
$\mathcal{U}_p$								
64	3.2120e-4		1.1811e-4		1.7072e-6		6.9825e-9	
144	9.9778e-5	2.8835	3.6707e-5	2.8823	3.4918e-7	3.9141	9.6881e-9	4.8712
256	4.3103e-5	2.9177	1.5858e-5	2.9174	1.1243e-7	3.9391	2.3000e-9	4.9986
400	2.2385e-5	2.9362	8.2350e-6	2.9367	4.6500e-8	3.9568	7.6067e-10	4.9585

Example 3.6.

In this example, we shall validate the superconvergence properties for nonlinear reaction problems by considering the nonlinear problem

$$u_x + 2u + u^2 = f(x,y), \qquad (x,y) \in \Omega = [0,1]^2, \tag{3.199a}$$

subject to the boundary conditions

$$u(0,y) = g(y). \tag{3.199b}$$

We select $f(x,y)$ and g such that the exact solution is

$$u(x,y) = \sqrt{1 + x^2 + 5\,y^2}. \tag{3.199c}$$

We solve this problem using triangular meshes obtained by subdividing $[0,1]^2$ into $n \times n$, $n = 4, 6, 8, 10$, squares and each square is subdivided into two triangles using the diagonal connecting the left-upper vertex to the right-lower vertex. We use the spaces $\mathcal{P}_p$, $\mathcal{V}_p$ and $\mathcal{U}_p$, $p = 0, 1, 2, 3$ and we plot the zero-level curves of the error in Figure 3.23. We also show the maximum errors at the superconvergence points in Table 3.13 which indicate that the DG solution is $O(h^{p+2})$ superconvergent at the roots of $(p+1)$-degree Legendre polynomial and at additional interior points for the spaces $\mathcal{V}_p$ and $\mathcal{U}_p$. We also observe that the zero-level curves of the error pass through the superconvergence points marked by $\times$. Thus, our superconvergence results extend to some nonlinear problems.

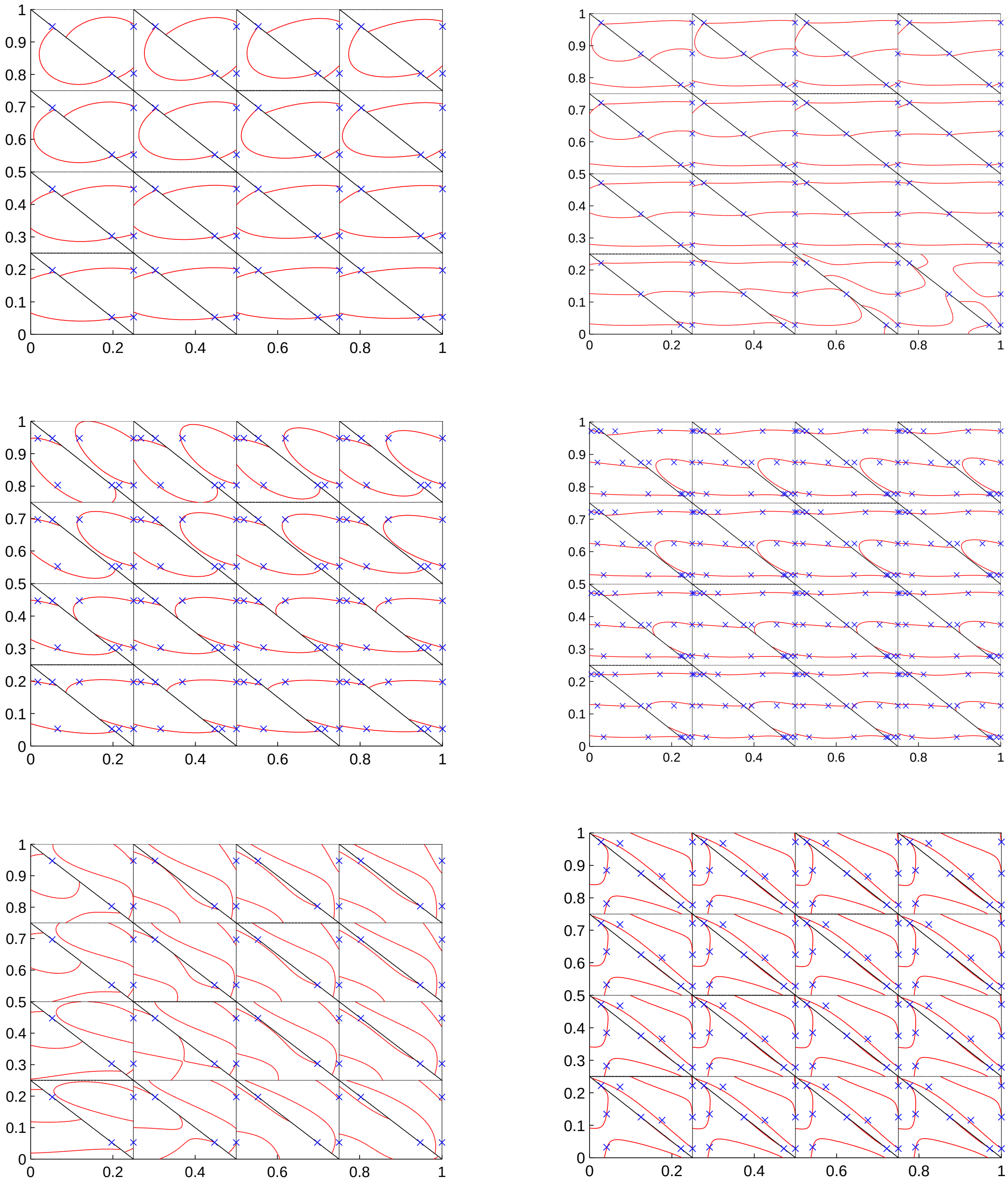

Figure 3.23: Zero-level curves of the true error for Example 3.6 on uniform meshes having $N = 32$ elements using $\mathcal{P}_1, \mathcal{V}_1, \mathcal{U}_1$, (left) and $\mathcal{P}_2, \mathcal{V}_2, \mathcal{U}_2$, (right). The superconvergence points are marked by $\times$.

Table 3.13: Maximum error and order of convergence at the superconvergence points for Example 3.6 on uniform meshes having $N = 32, 72, 128, 200$ elements.

	$\mathcal{P}_p$							
N	$p=0$		$p=1$		$p=2$		$p=3$	
	$\|\|e\|\|_\infty^*$	order	$\|\|e\|\|_\infty^*$	order	$\|\|e\|\|_\infty^*$	order	$\|\|e\|\|_\infty^*$	order
32	1.3915e-2		8.0268e-4		6.6220e-6		1.3806e-6	
72	6.3972e-3	1.9166	2.4327e-4	2.9442	1.3329e-6	3.9535	1.8998e-7	4.8915
128	3.6819e-3	1.9202	1.0404e-4	2.9525	4.2550e-7	3.9691	4.6231e-8	4.9126
200	2.3981e-3	1.9213	5.3815e-5	2.9542	1.7518e-7	3.9769	1.5475e-8	4.9044
	$\mathcal{V}_p$							
32	1.3915e-2		2.2779e-4		8.3106e-6		1.0274e-6	
72	6.3972e-3	1.9166	6.8233e-5	2.9731	1.6922e-6	3.9250	1.4123e-7	4.8941
128	3.6819e-3	1.9202	2.9153e-5	2.9559	5.4496e-7	3.9386	3.4102e-8	4.9396
200	2.3981e-3	1.9213	1.5044e-5	2.9647	2.2566e-7	3.9511	1.1373e-8	4.9208
	$\mathcal{U}_p$							
32	8.0268e-4		2.3919e-4		6.6582e-6		3.0642e-7	
72	2.4327e-4	2.9442	7.3413e-5	2.9130	1.3410e-6	3.9519	4.0877e-8	4.9680
128	1.0404e-4	2.9525	3.1778e-5	2.9105	4.2874e-7	3.9639	9.8312e-9	4.9534
200	5.3815e-5	2.9542	1.6553e-5	2.9227	1.7698e-7	3.9652	3.2666e-9	4.9376

3.8 Conclusion

We investigated higher-order DG methods for hyperbolic problems on triangular meshes. We studied the effect of finite element spaces on the superconvergence properties of DG solutions on three types of triangular elements. We showed that the DG solution is $O(h^{p+2})$ superconvergent at Legendre points on the *outflow* edge on triangles having one *outflow* edge using three polynomial spaces. On elements of type I the DG solution is $O(h^{p+2})$ superconvergent at the vertices of the *inflow* edge for an augmented space $\mathcal{U}_p$. Furthermore, we discovered additional superconvergence points in the interior of triangles. Finally, we established a global superconvergence result on meshes consisting of triangles of type III only. Superconvergence on more general meshes and nonlinear problems as well as *a posteriori* error estimates based on these superconvergence results will be presented in the next chapter.